



Phenomenology of multi-hadron and jet production in heavy ion collisions at Large Hadron Collider

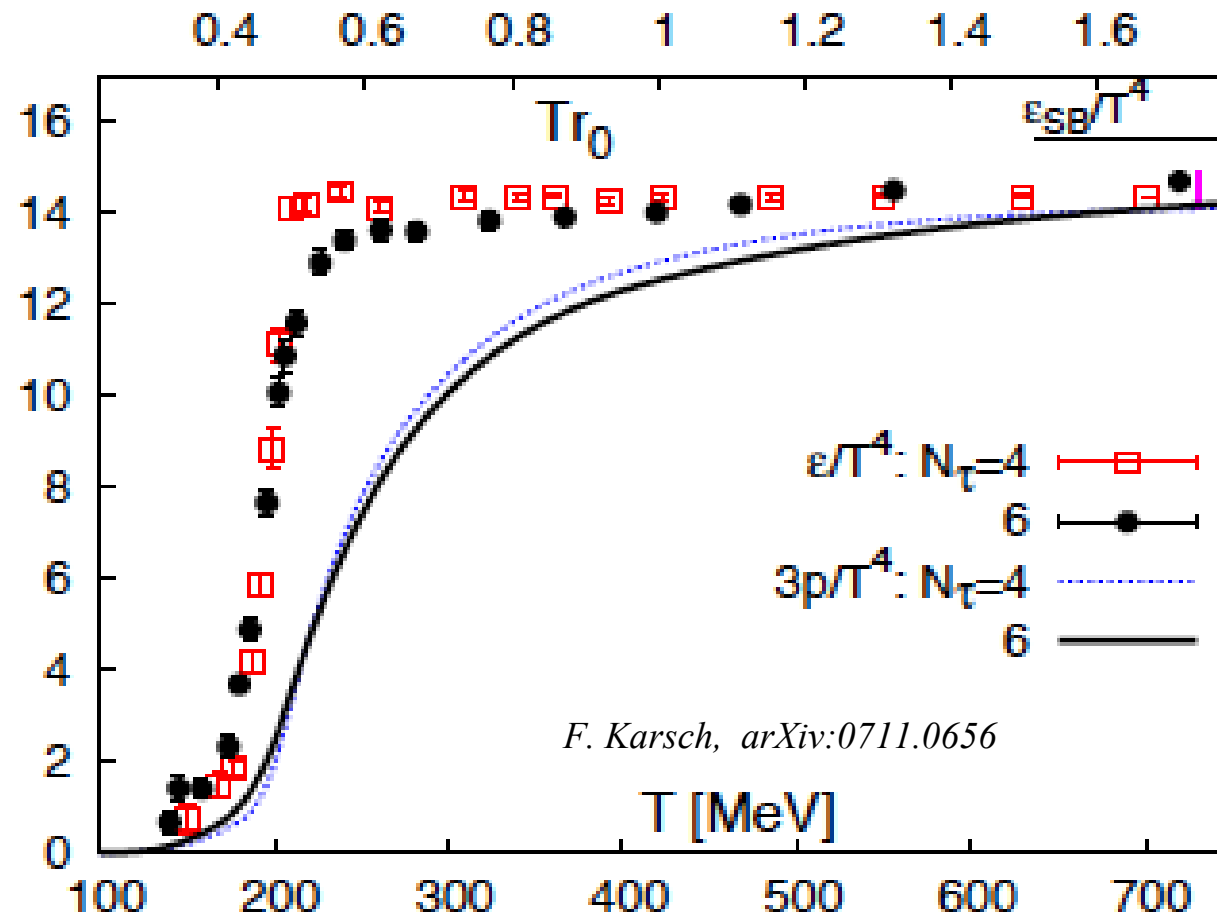


I.P. Lokhtin

Skobeltsyn Institute of Nuclear Physics,
Lomonosov Moscow State University

*The XXII International Workshop «High Energy Physics and Quantum Field Theory»
June 24–July 1, 2015, Samara, Russia*

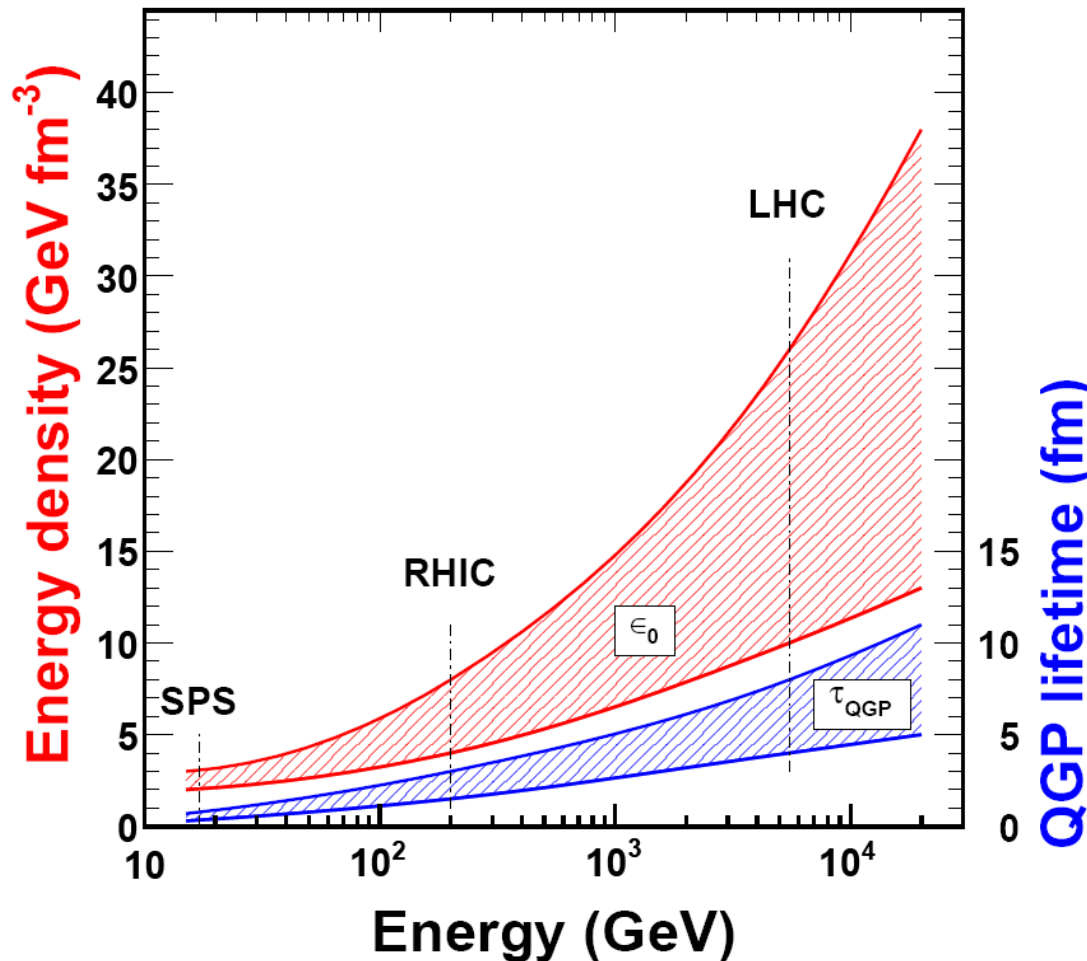
Deconfinement of nuclear matter



*Deconfinement of nuclear matter and quark-gluon matter (QGM) formation –
the prediction of Lattice Quantum Chromodynamics (QCD) for systems
with high enough temperature and/or baryon density*

Study of quark-gluon matter in relativistic heavy ion collisions

SPS (CERN) → RHIC (BNL) → LHC (CERN)



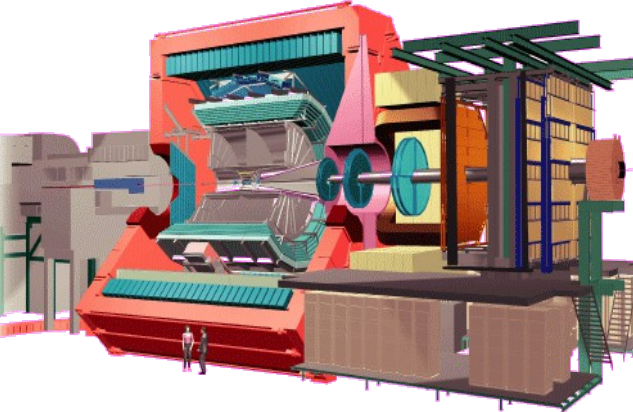
Heavy ion physics at the LHC

2010, 2011: PbPb ($\sqrt{s_{NN}} = 2.76 \text{ TeV}$);

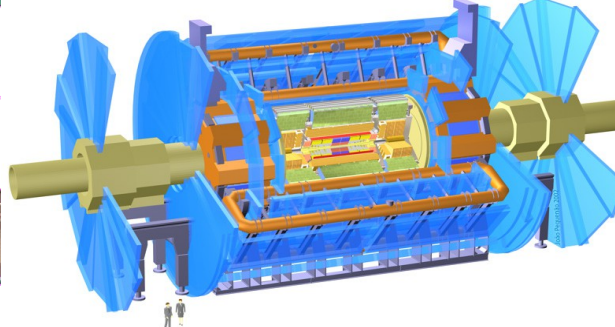
2012/2013: pPb ($\sqrt{s_{NN}} = 5.02 \text{ TeV}$); ≥ 2015 : PbPb ($\sqrt{s_{NN}} = 5.1\text{-}5.5 \text{ TeV}$);...

New regime of heavy ion physics with the important role of hard QCD-processes in hot and long-lived quark-gluon medium
complementary measurements from ALICE & CMS/ATLAS

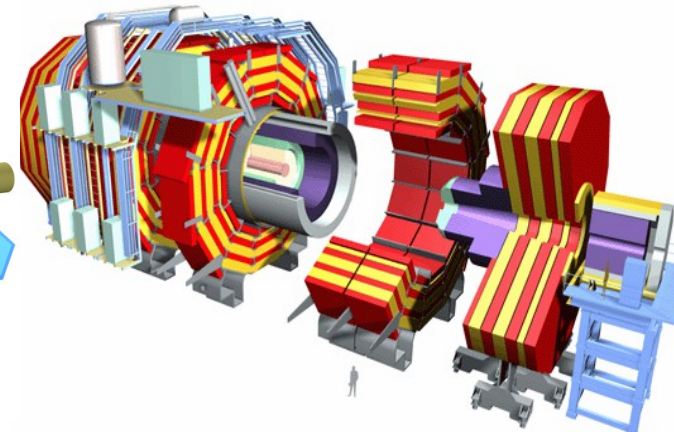
ALICE



ATLAS



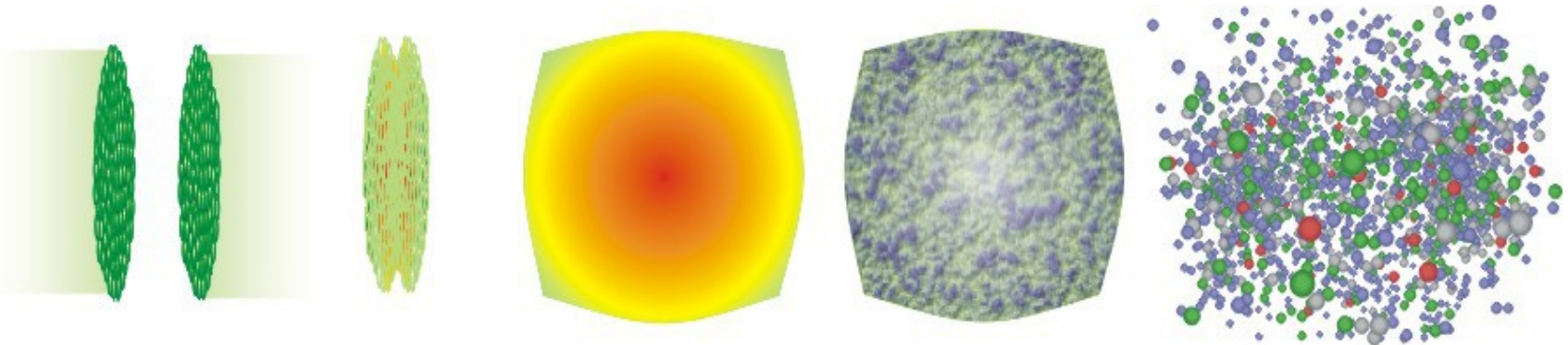
CMS



ALICE (low- p_T charged particle tracking, hadron ID, central e , forward μ (J/ψ , Υ), soft γ ,...)
soft probes + selected hard probes

CMS/ATLAS (high- p_T charged particle tracking, central μ (J/ψ , Υ , Z , W), hard γ , calorimetric jets...)
hard probes + selected soft probes

Basic probes of hot and dense quark-gluon matter formation in PbPb collisions at Large Hadron Collider at $\sqrt{s}_{\text{NN}} = 2.76 \text{ TeV}$



Hydrodynamical (collective) properties of multi-particle system

- Anisotropic flow
- Two-particle azimuthal correlations (“ridge”)

Medium-induced energy loss of hard quarks and gluons (“jet quenching”)

- Transverse momentum imbalance in jet+jet , $\gamma+\text{jet}$, $Z+\text{jet}$ production
- Suppression of hard hadron and jet yields
- Modification of internal jet structure

Debye screening of colour charge and thermal charmonium production

- Specific pattern of quarkonium suppression (J/ψ , Υ)
- Regeneration and anisotropic flow of J/ψ mesons

HYDJET and HYDJET++ relativistic heavy ion event generators

HYDJET (HYDrodynamics + JETs) - event generator to simulate heavy ion event as merging of two independent components (soft hydro-type part + hard multi-partonic state, the latter is based on PYQUEN - PYthia QUENched).

<http://cern.ch/lokhtin/hydro/hydjett.html>

(latest version 1.9)

Original paper: I.Lokhtin, A.Snigirev, Eur. Phys. J. C 46 (2006) 2011

HYDJET++ (HYDJET v.2.*) – continuation of HYDJET (identical hard component + improved soft component including full set of thermal resonance production).

<http://cern.ch/lokhtin/hydjetpp.html>

(latest version 2.2)

Original paper: I.Lokhtin, L.Malinina, S.Petrushanko, A.Snigirev, I.Arsene,
K.Tywoniuk, Comp. Phys. Comm. 180 (2009) 779

HYDJET++ (soft component): physics frames

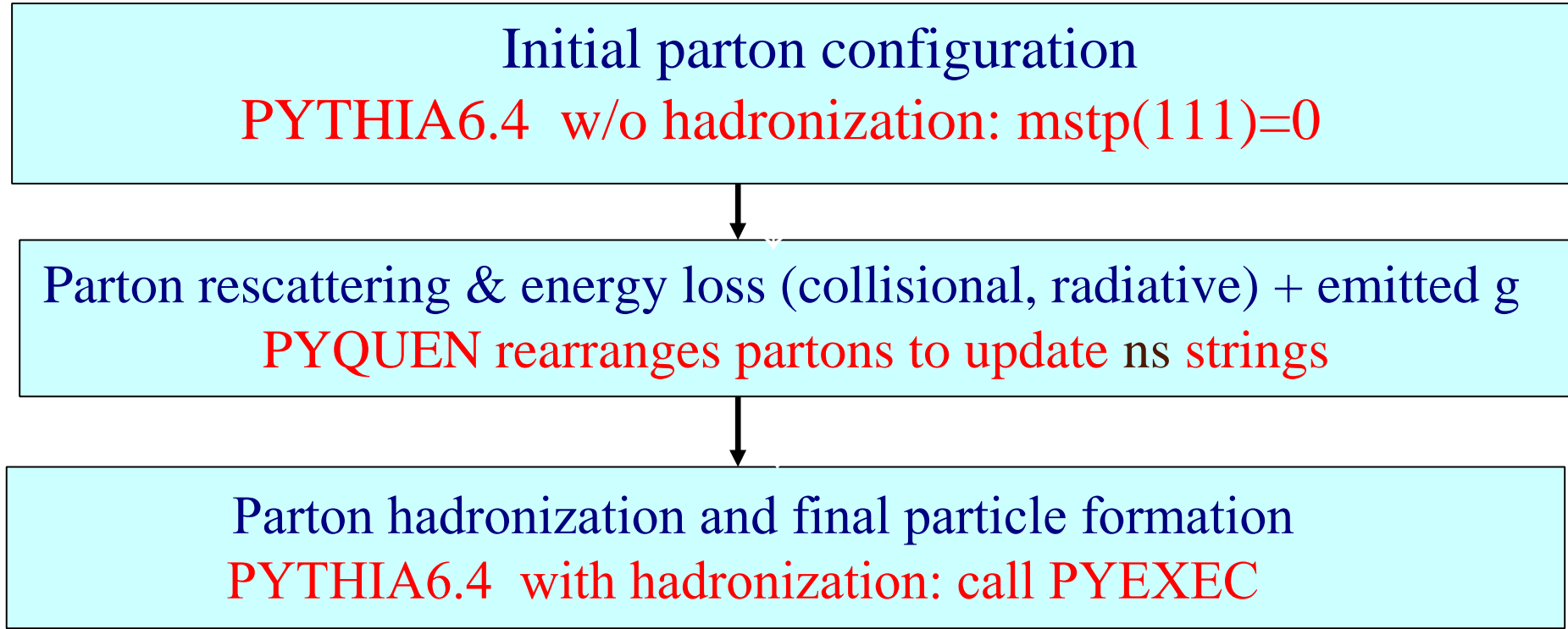
Soft (hydro) part of HYDJET++ is based on the adapted FAST MC model:

Part I: *N.S.Amelin, R.Lednisky, T.A.Pocheptsov, I.P.Lokhtin, L.V.Malinina, A.M.Snigirev, Yu.A.Karpenko, Yu.M.Sinyukov, Phys. Rev. C 74 (2006) 064901*

Part II: *N.S.Amelin, R.Lednisky, I.P.Lokhtin, L.V.Malinina, A.M.Snigirev, Yu.A.Karpenko, Yu.M.Sinyukov, I.C.Arsene, L.Bravina, Phys. Rev. C 77 (2008) 014903*

- ✓ fast HYDJET-inspired MC procedure for soft hadron generation
- ✓ multiplicities are determined assuming thermal equilibrium
- ✓ hadrons are produced on the hypersurface represented by a parameterization
 - of relativistic hydrodynamics with given freeze-out conditions
- ✓ chemical and kinetic freeze-outs are separated
- ✓ decays of hadronic resonances are taken into account (360 particles from SHARE data table) with “home-made” decayer
- ✓ written within ROOT framework (C++)
- ✓ contains 16 free parameters (but this number may be reduced to 9)

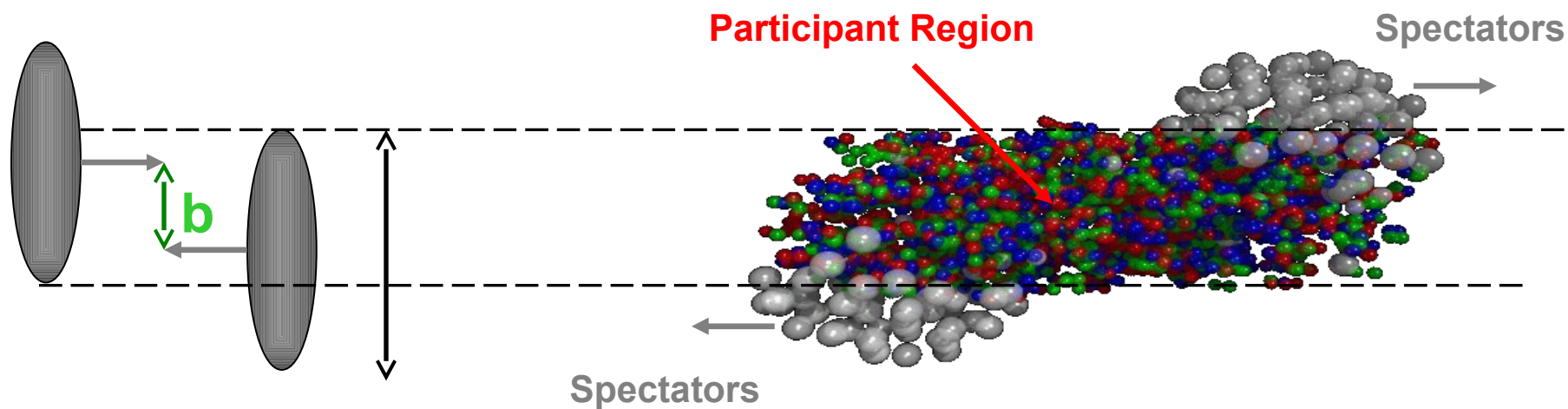
HYDJET++ (hard component): PYQUEN (PYthia QUENched)



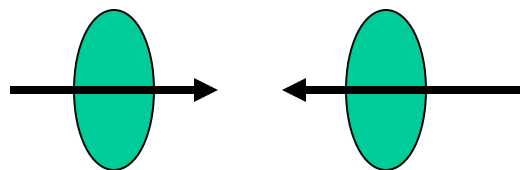
Three model parameters: initial maximal QGP temperature T_0 , QGP formation time τ_0 and number of active quark flavors in QGP N_f

(+ minimal p_T of hard process $Ptmin$ to specify the number of hard NN collisions)
₈

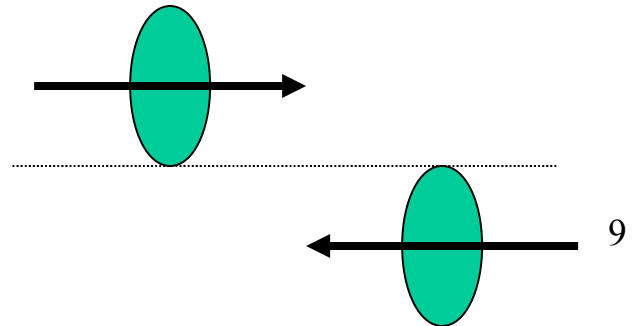
Centrality of nucleus-nucleus interactions



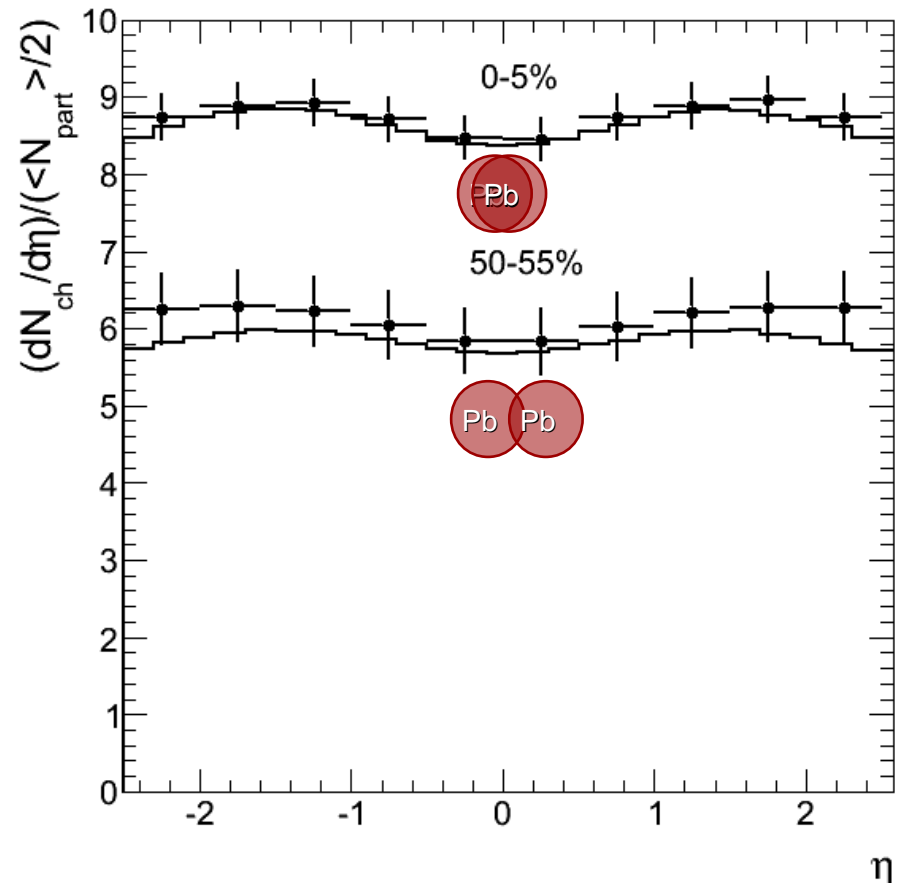
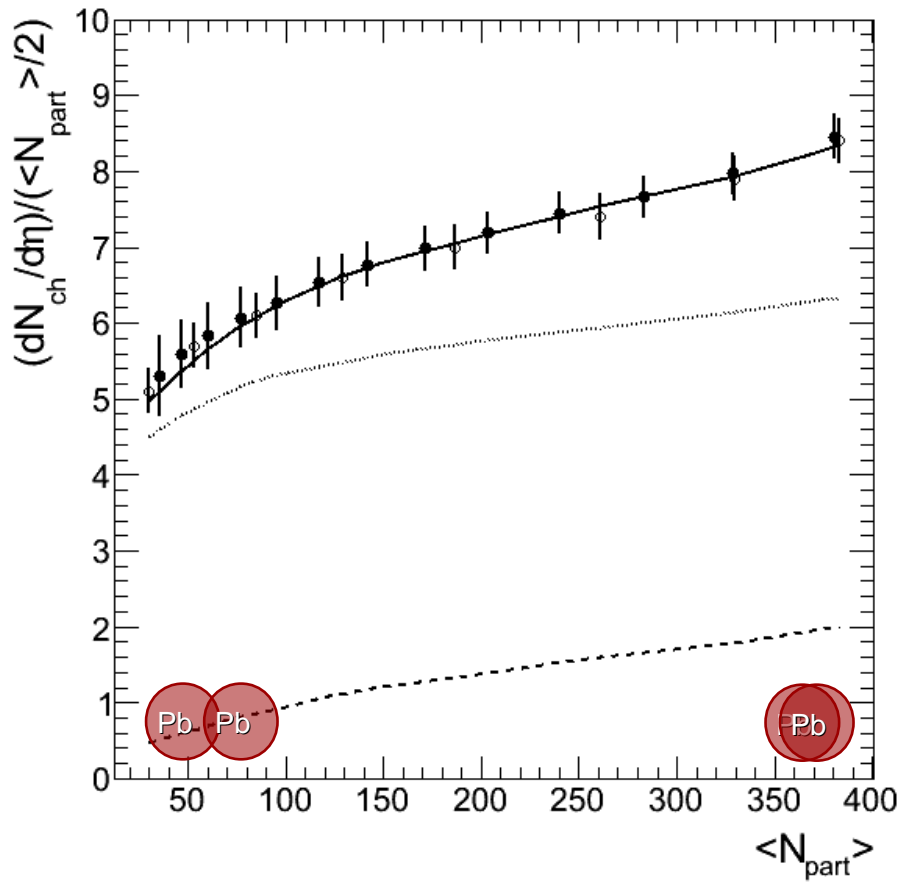
central collision



peripheral collision



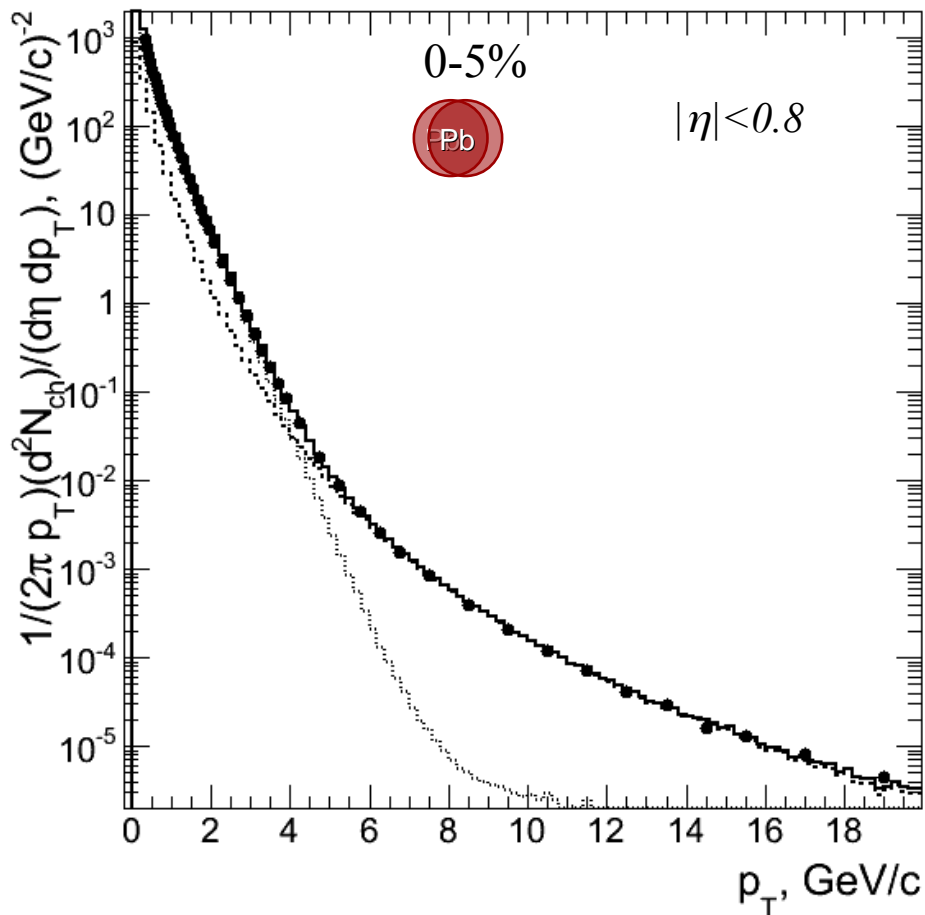
Charged multiplicity vs. centrality and pseudorapidity



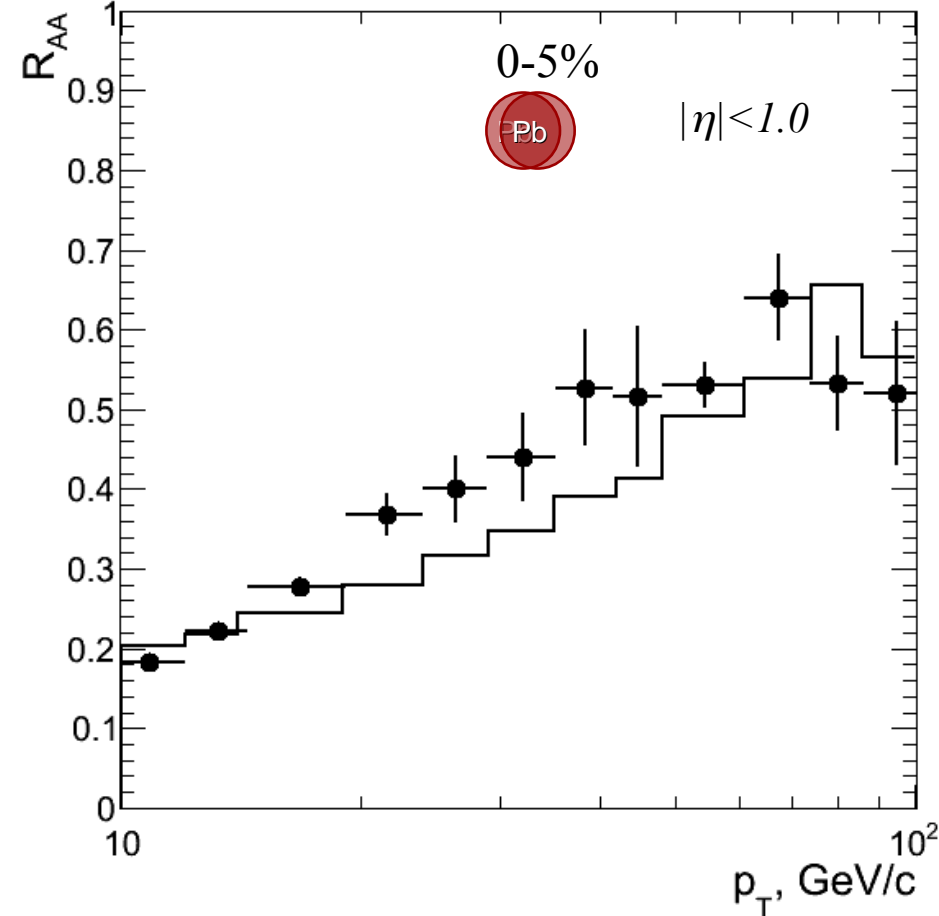
Open points: ALICE data (*PRL 106 (2011) 032301*), closed points: CMS data (*JHEP 1108 (2011) 141*);
histograms: HYDJET++

Tuned HYDJET++ reproduces multiplicity vs. event centrality (down to very peripheral events)
with contribution of hard component to multiplicity in mid-rapidity 10
for central PbPb $\sim 30\%$, as well as approximately flat pseudorapidity distribution.

P_T -spectrum and nuclear modification factor R_{AA} for inclusive charged hadrons



$$R_{AA} = \frac{\sigma_{pp}^{inel}}{\langle N_{coll} \rangle} \frac{d^2 N_{AA} / dp_T d\eta}{d^2 \sigma_{pp} / dp_T d\eta} \sim \frac{\text{"QCD Medium"}}{\text{"QCD Vacuum"}}$$

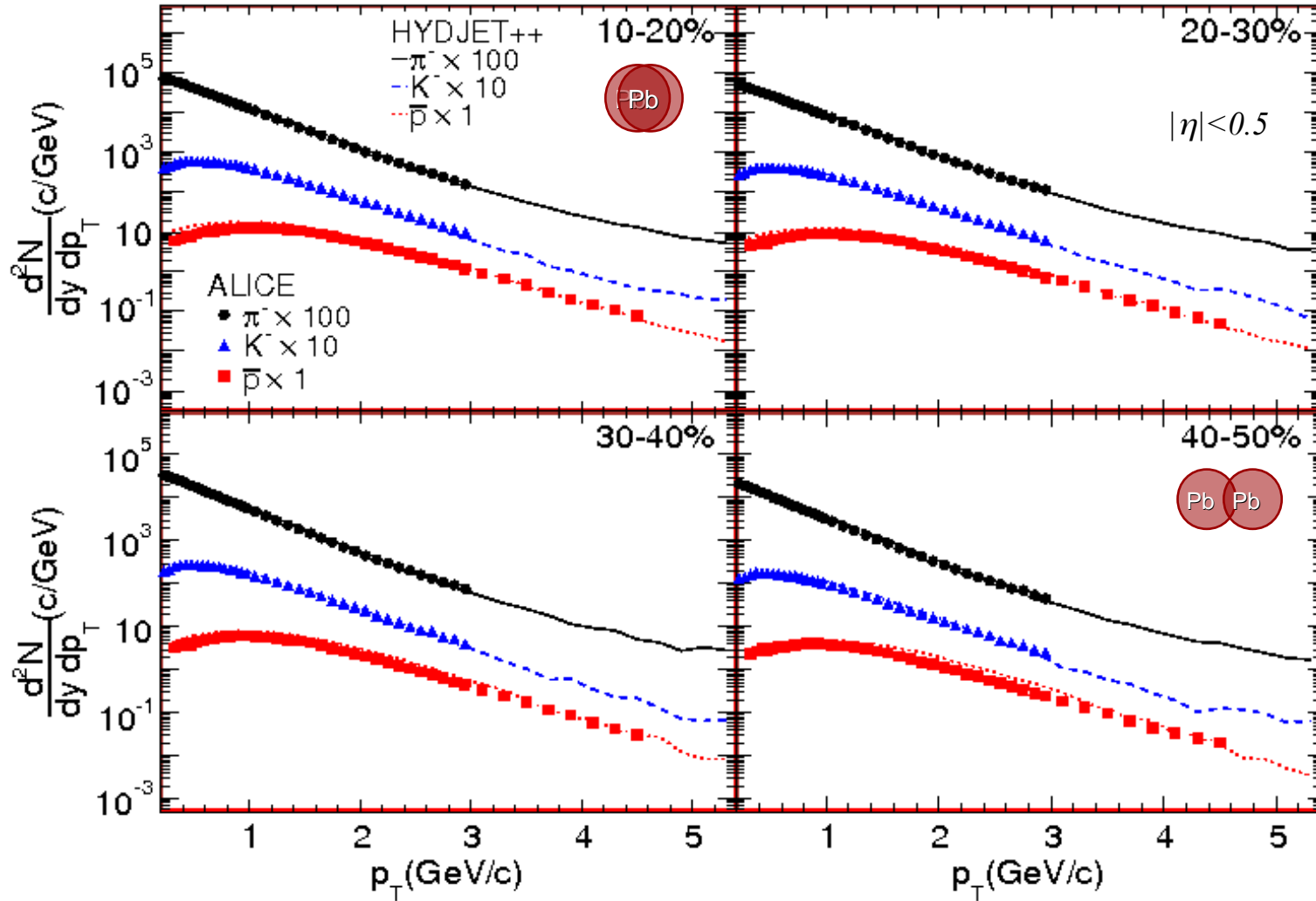


$R_{AA} > 1$: enhancement
 $R_{AA} = 1$: no medium effect
 $R_{AA} < 1$: suppression

Points: ALICE (left) (*PLB 696 (2011) 30*) & CMS (right) (*EPJC 72 (2012) 1945*) data;
histograms: HYDJET++

HYDJET++ reproduces p_T -spectrum and R_{AA} for central PbPb in mid-rapidity up to $p_T \sim 100$ GeV/c

P_T -spectra of identified hadrons

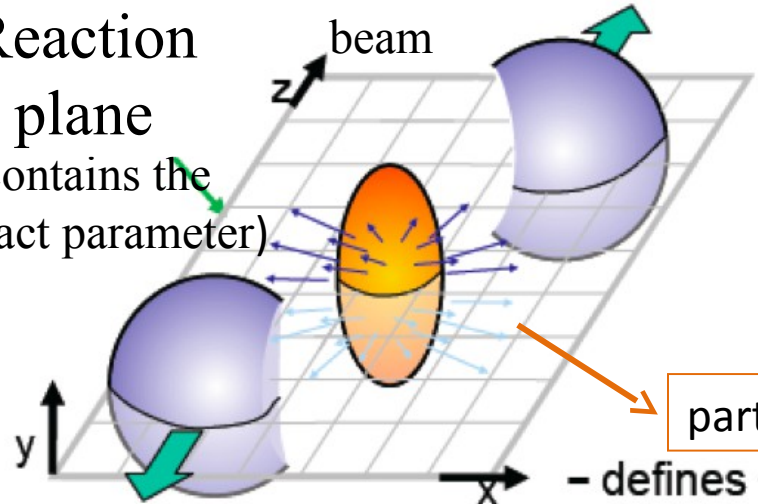


Points: ALICE data (APP B 43 (2012) 555); histograms: HYDJET++

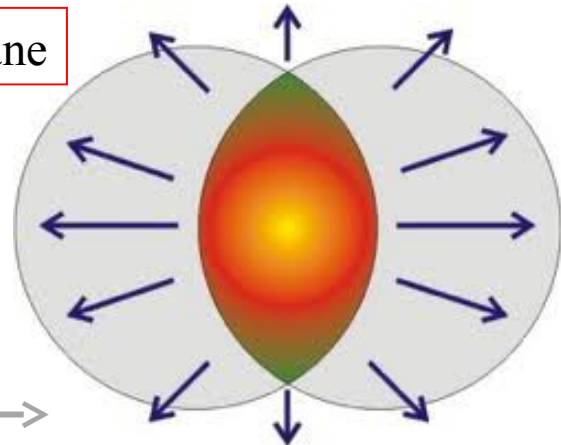
HYDJET++ reproduces p_T -spectrum of pions, kaons and (anti-)protons as well ¹²

Azimuthal correlations and flow

Reaction plane
(contains the impact parameter)



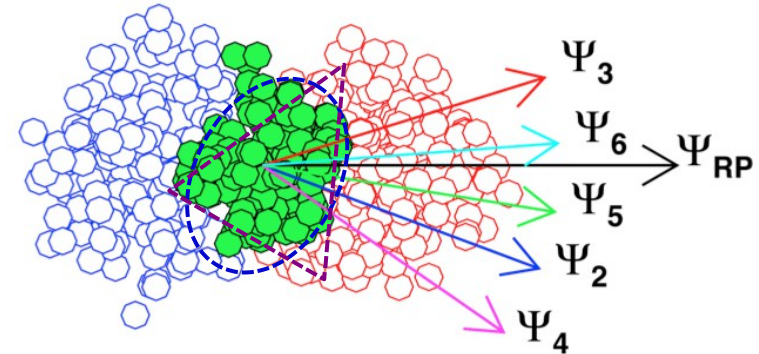
Event plane



Elliptic flow

Triangular flow

$$\frac{dN}{d\phi} \sim 1 + 2v_2 \cos 2(\phi - \Psi_2) + 2v_3 \cos 3(\phi - \Psi_3) + \dots$$



Anisotropic flow generation in HYDJET++ (soft component)

Elliptic flow v_2

- spatial modulation of freeze-out surface
- fluid velocity modulation

Spatial anisotropy

$$\epsilon(b) = \frac{R_y^2 - R_x^2}{R_y^2 + R_x^2},$$

$R(b)$ – surface radius

$$v_2 \propto \frac{2(\delta - \epsilon)}{(1 - \delta^2)(1 - \epsilon^2)}$$

Momentum anisotropy

$$\tan \varphi_u = \sqrt{\frac{1 - \delta(b)}{1 + \delta(b)}} \tan \varphi.$$

φ_u : azimuthal angle of fluid velocity

φ : spatial azimuthal angle

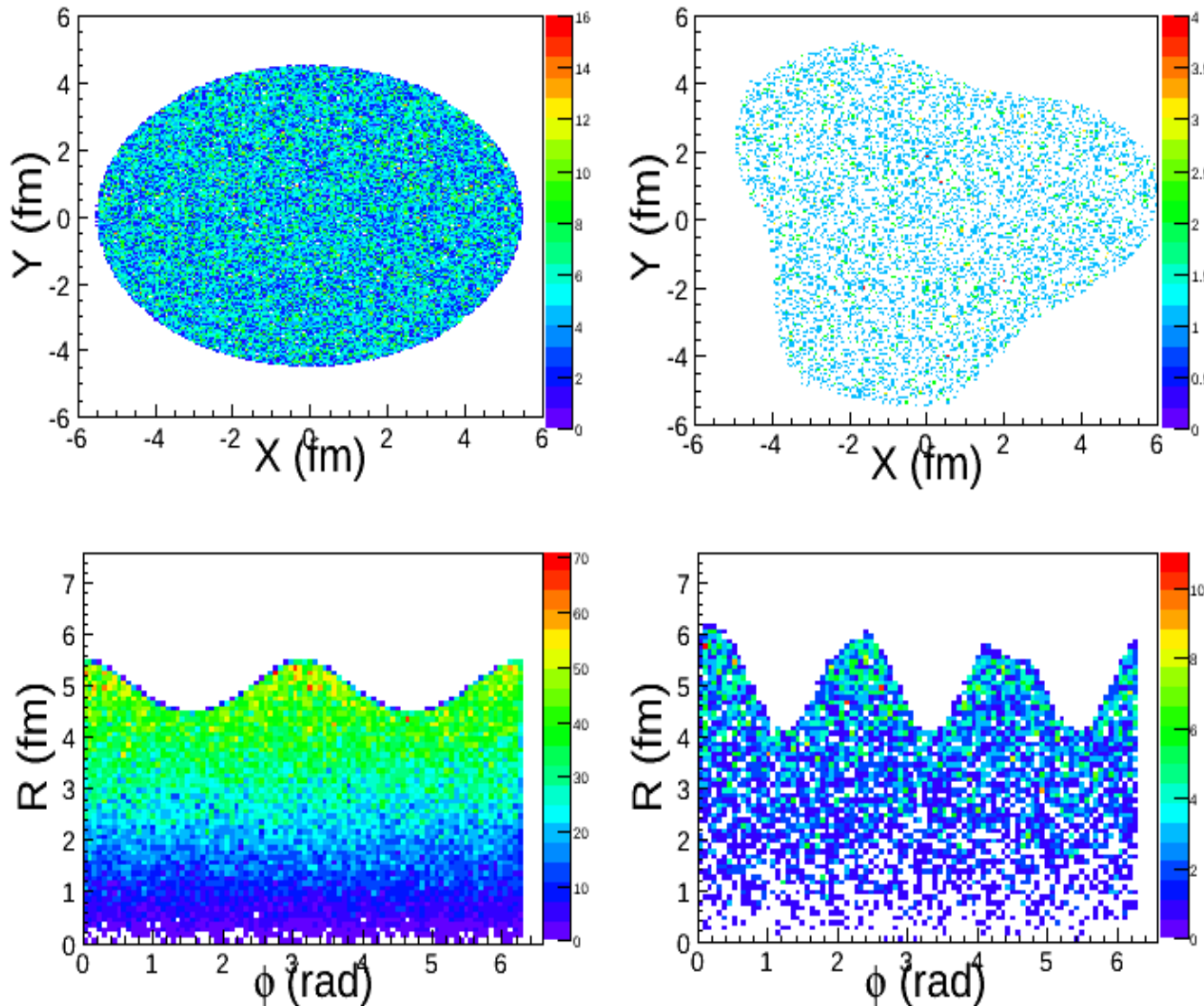
Triangular flow v_3

Spatial modulation of freeze-out surface as $\cos(3\varphi)$ with independent phase Ψ_3 and parameter ϵ_3

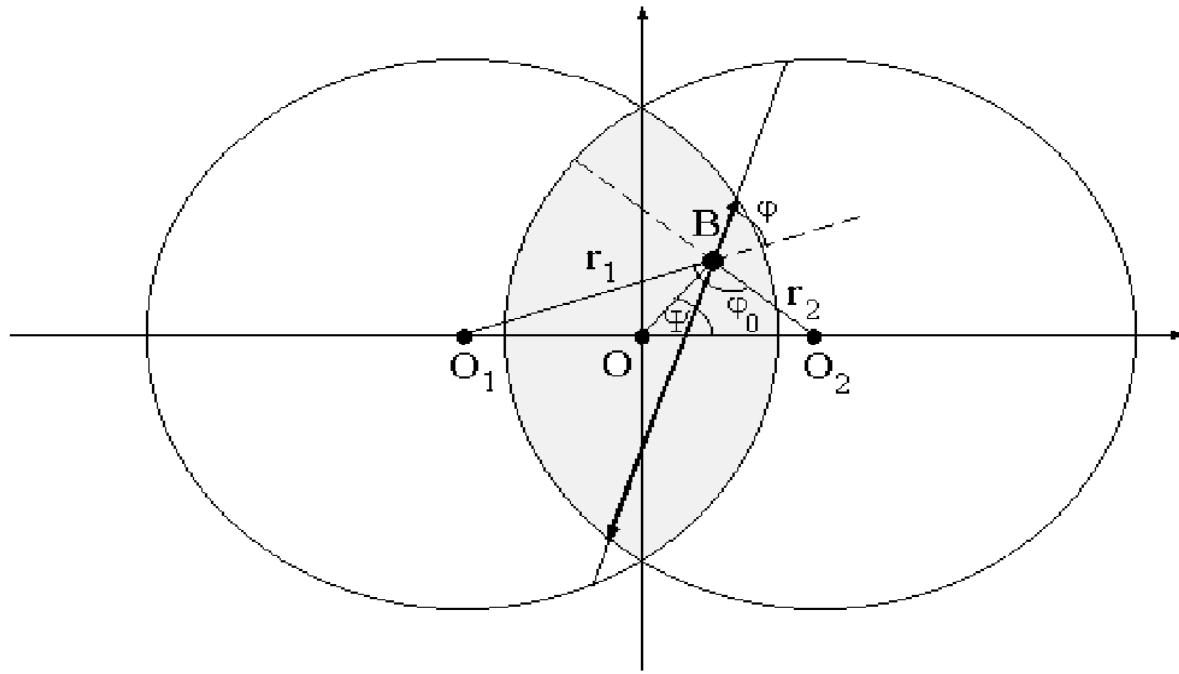
$$R(b, \phi) = R_f(b) \frac{\sqrt{1 - \epsilon^2(b)}}{\sqrt{1 + \epsilon(b) \cos 2\phi}} [1 + \epsilon_3(b) \cos 3(\phi + \Psi_3^{\text{RP}})]$$

Three parameters $\epsilon(b_0)$, $\epsilon_3(b_0)$ и $\delta(b_0)$ is tuned to fit the data

Anisotropic flow generation in HYDJET++ (soft component)

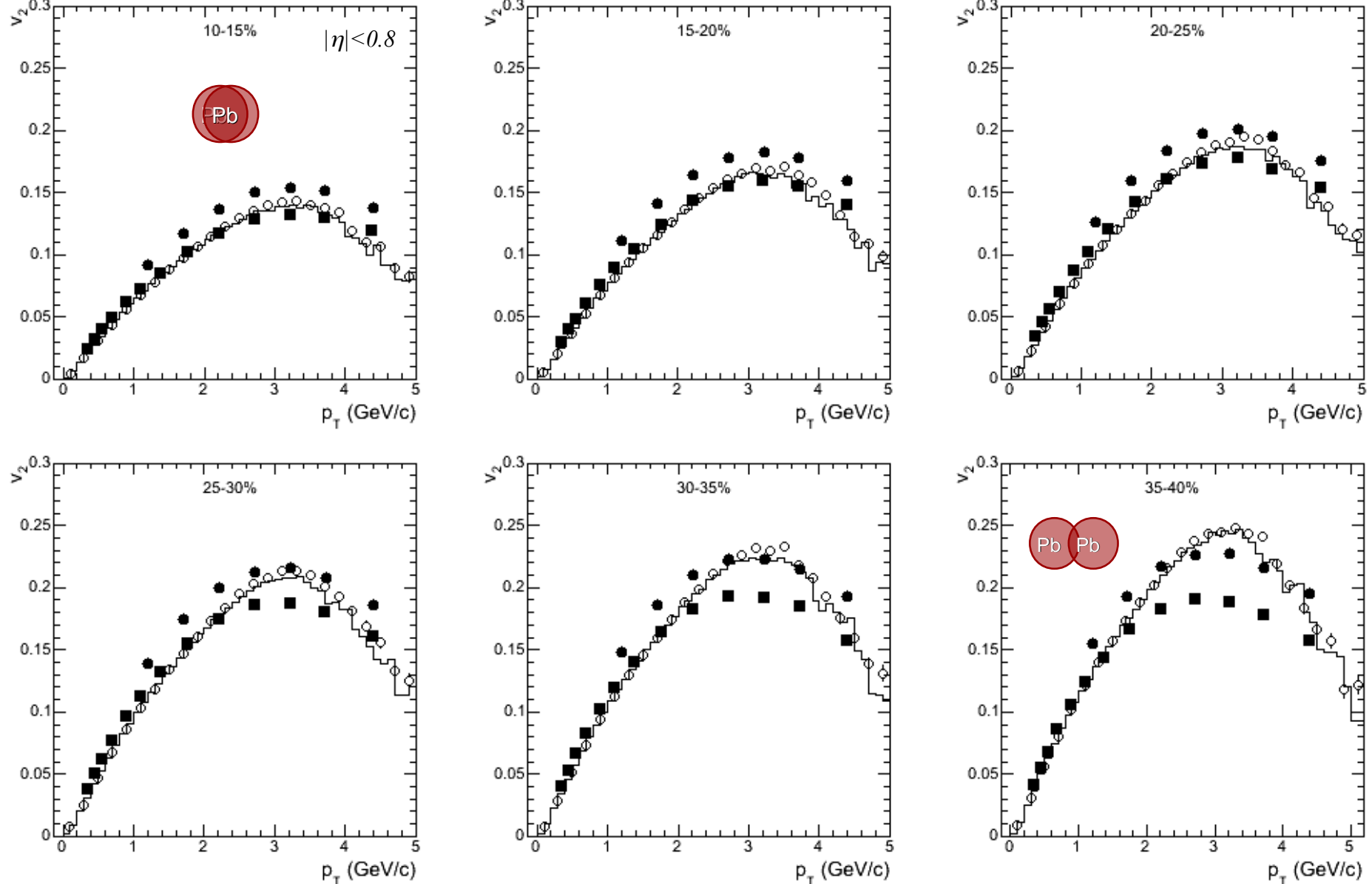


Anisotropic flow generation in HYDJET++ (hard component)



Some anisotropic flow for hard component (v_2 and higher even harmonics at high transverse momenta) is generated due to partonic rescattering and energy loss in azimuthally-asymmetric volume of the medium

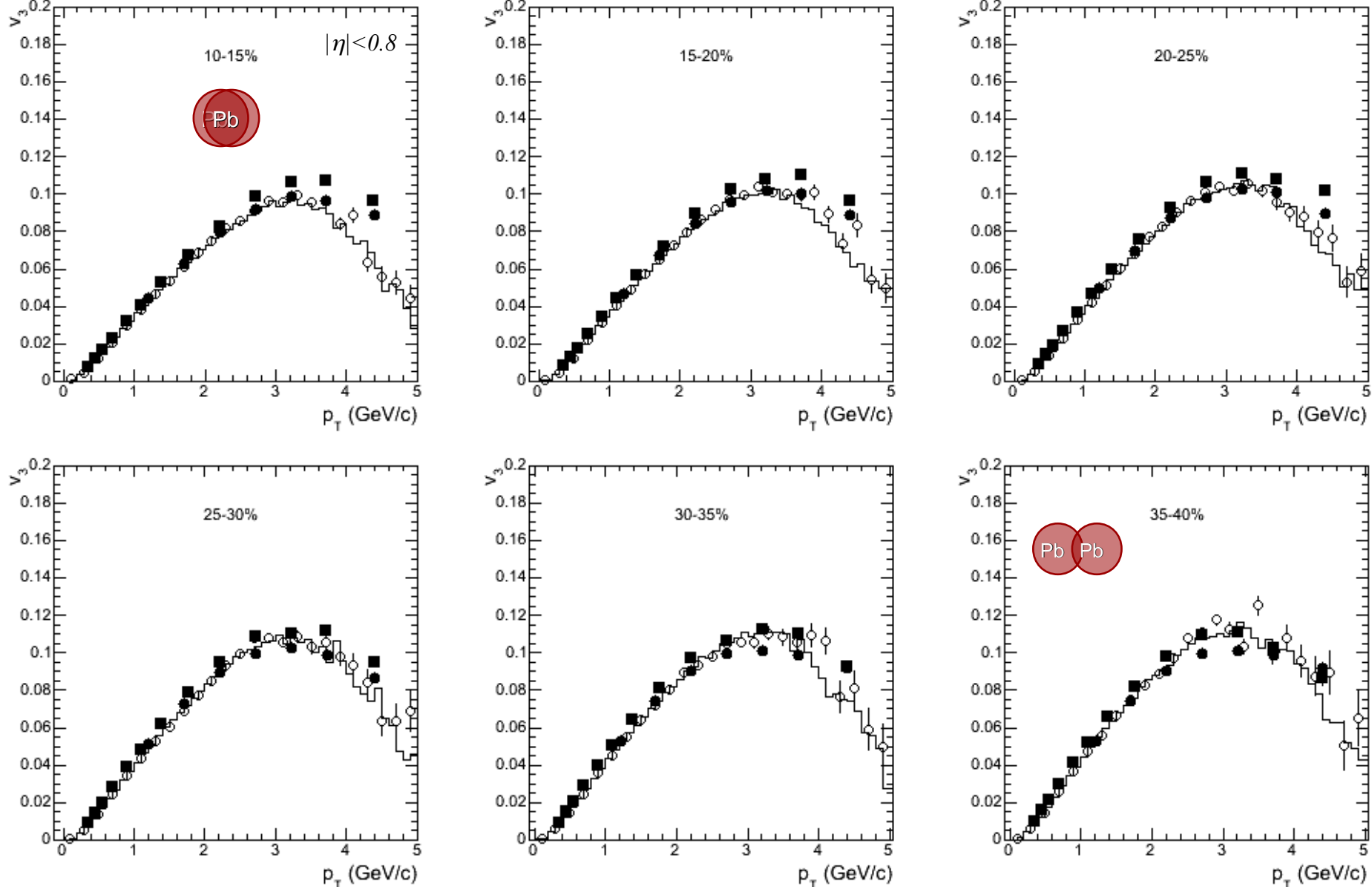
Elliptic flow of inclusive charged hadrons



Closed circles and squares: CMS data $v_2\{2\}$ & $v_2\{\text{LYZ}\}$ (*PRC 87 (2013) 014902*);

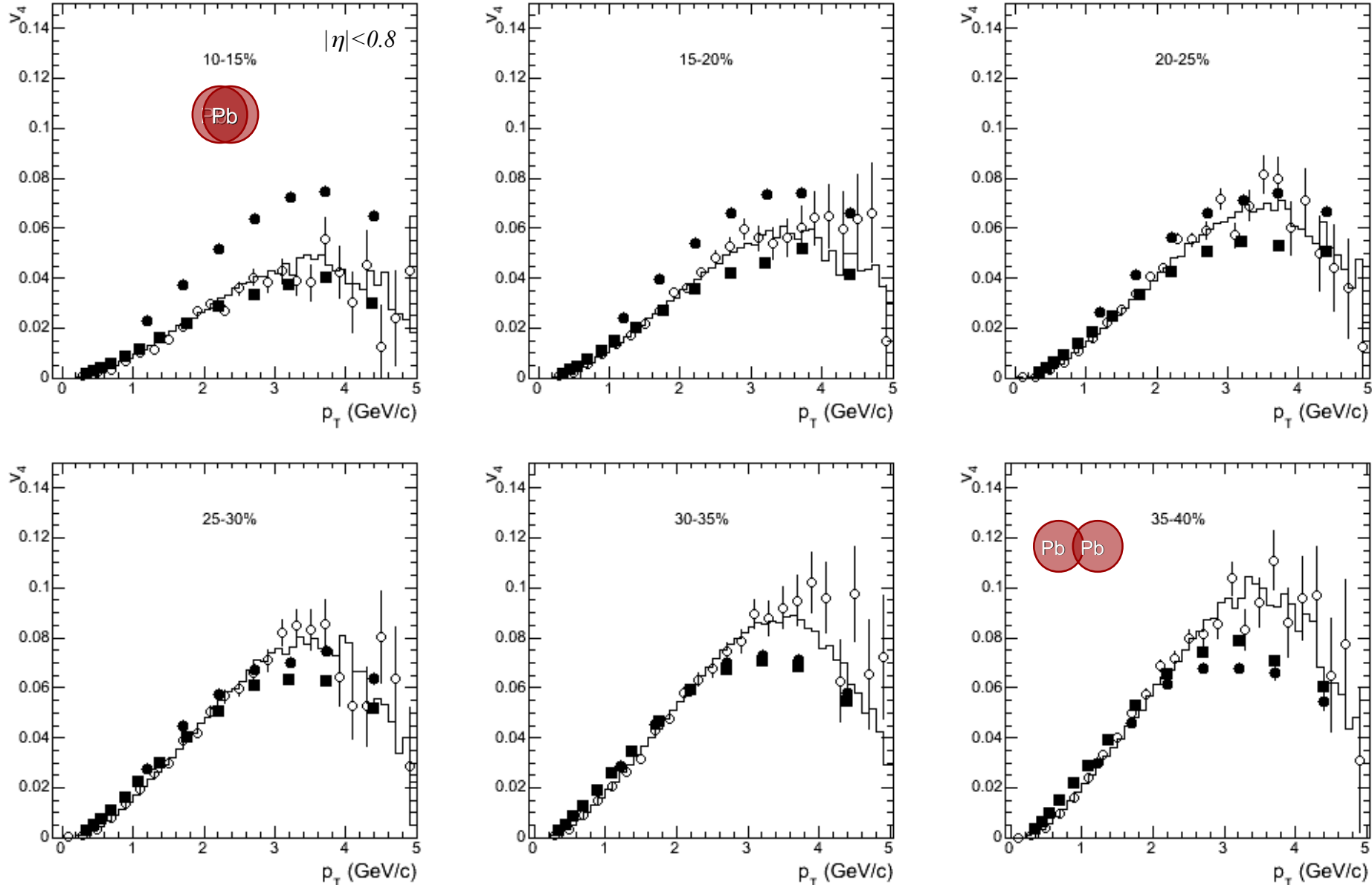
histograms and open circles: HYDJET++ (“true” $v_2(\psi_2)$ & $v_2\{\text{EP}\}$)

Triangular flow of inclusive charged hadrons



Closed circles and squares: CMS data $v_3\{2\}$ & $v_3\{\text{EP}\}$ (*PRC 89 (2014) 044906*);
 histograms and open circles: HYDJET++ (“true” $v_3(\psi_3)$ & $v_3\{\text{EP}\}$)

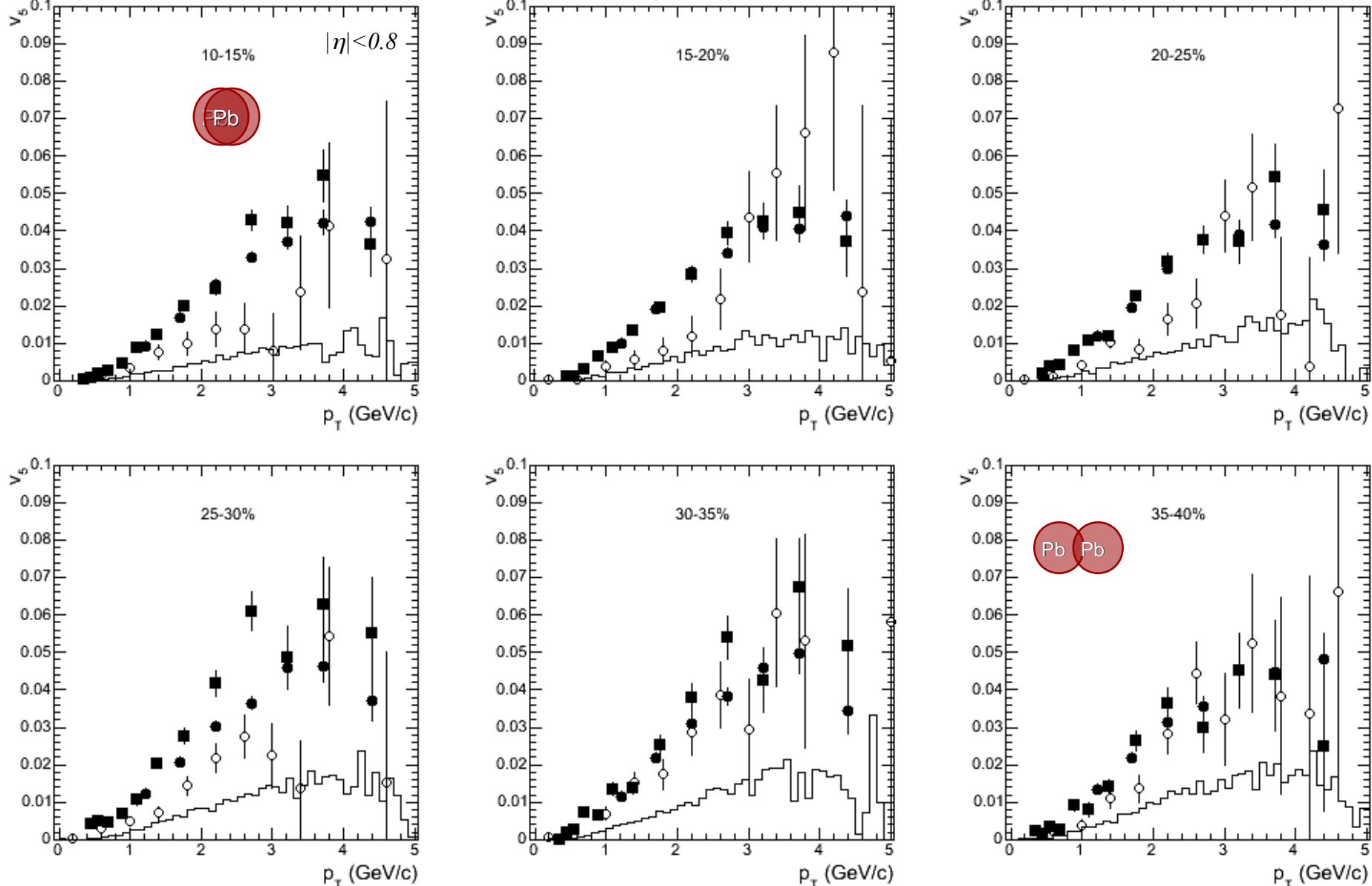
Quadrangular flow of inclusive charged hadrons



Closed circles and squares: CMS data $v_4\{\text{2}\}$ & $v_4\{\text{LYZ}\}$ (*PRC 89 (2014) 044906*);

histograms and open circles: HYDJET++ (“true” $v_4(\psi_2)$ & $v_4\{\text{EP}\}$)

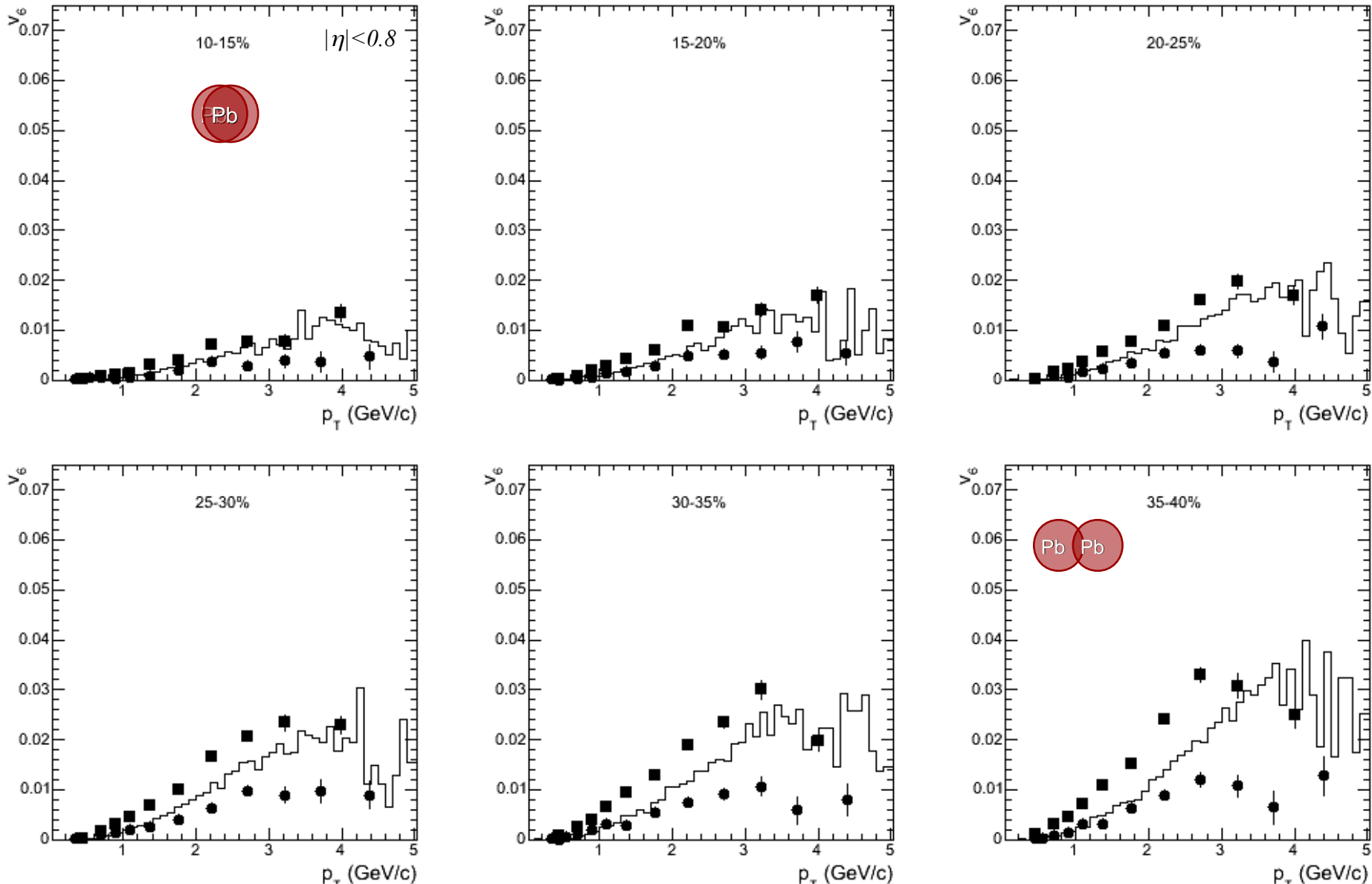
Pentagonal flow of inclusive charged hadrons



Closed circles and squares: CMS data $v_5\{2\}$ & $v_5\{\text{EP}\}$ (*PRC 89 (2014) 044906*);

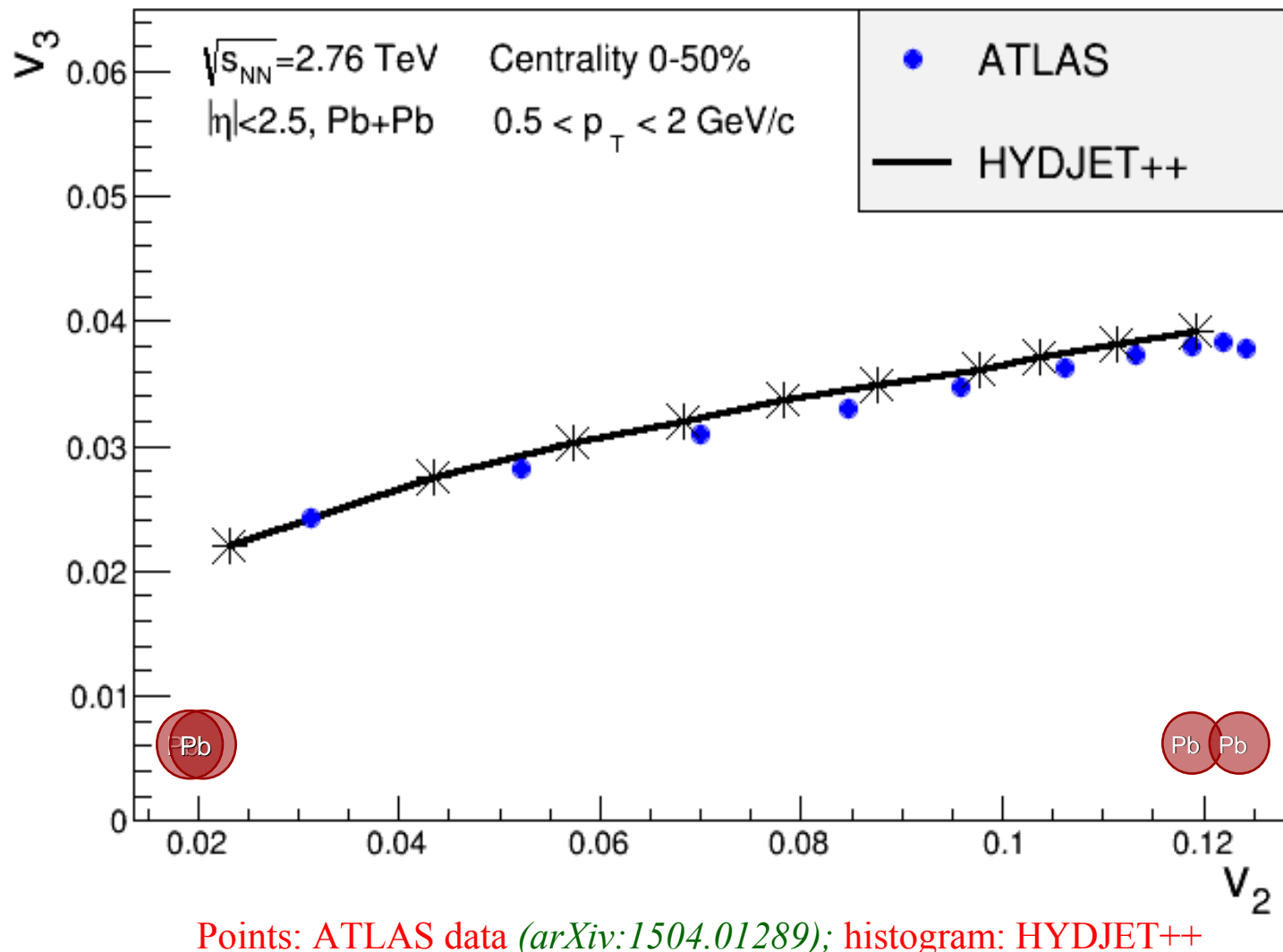
histograms and open circles: HYDJET++ (“true” $v_5(\psi_3)$ & $v_5\{\text{EP}\}$)

Hexagonal flow of inclusive charged hadrons



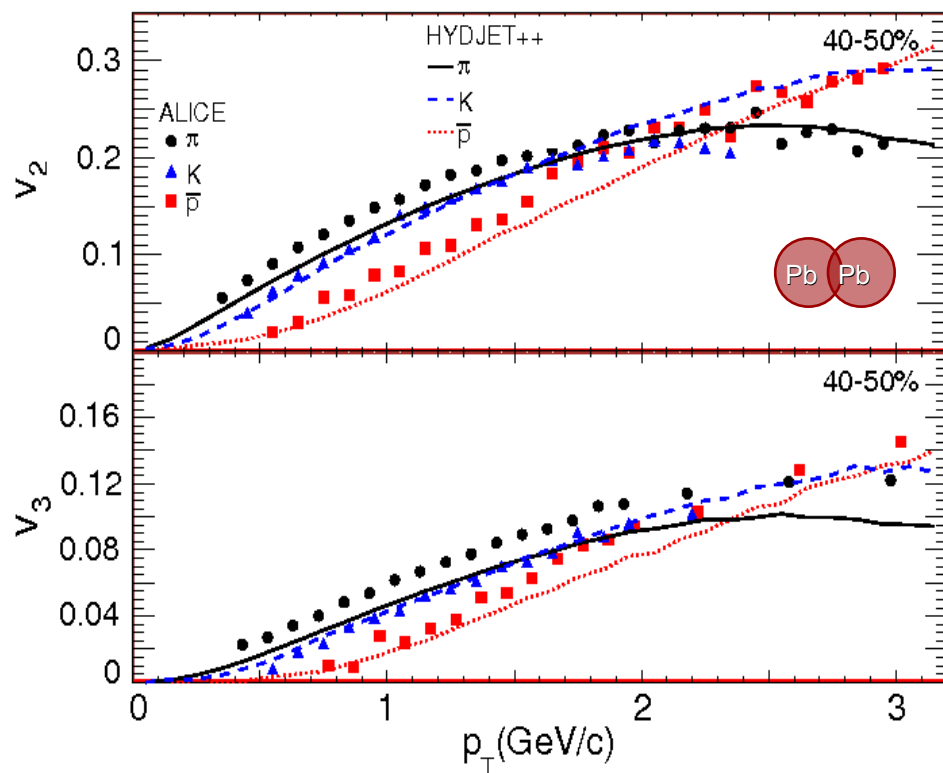
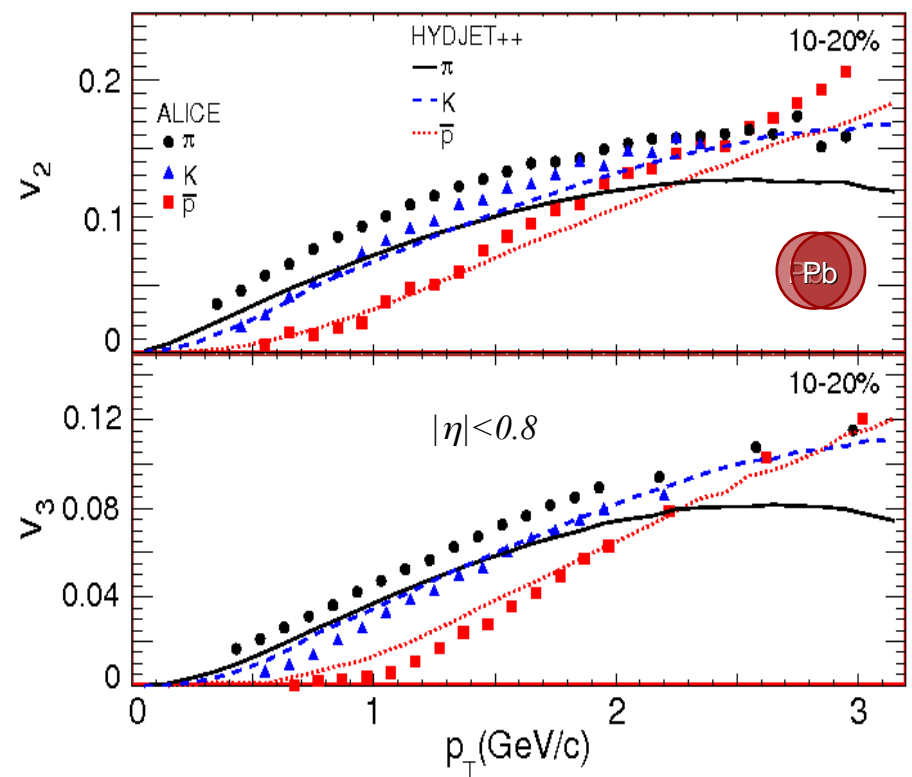
Closed circles and squares: CMS data $v_6\{\text{EP}/\psi_2\}$ & $v_6\{\text{LYZ}\}$ (*PRC 89 (2014) 044906*);
 histograms: HYDJET++ (“true” $v_6(\psi_2)$)

Correlations between elliptic and triangular flows



HYDJET++ reproduces the correlation between elliptic and triangular flows 22

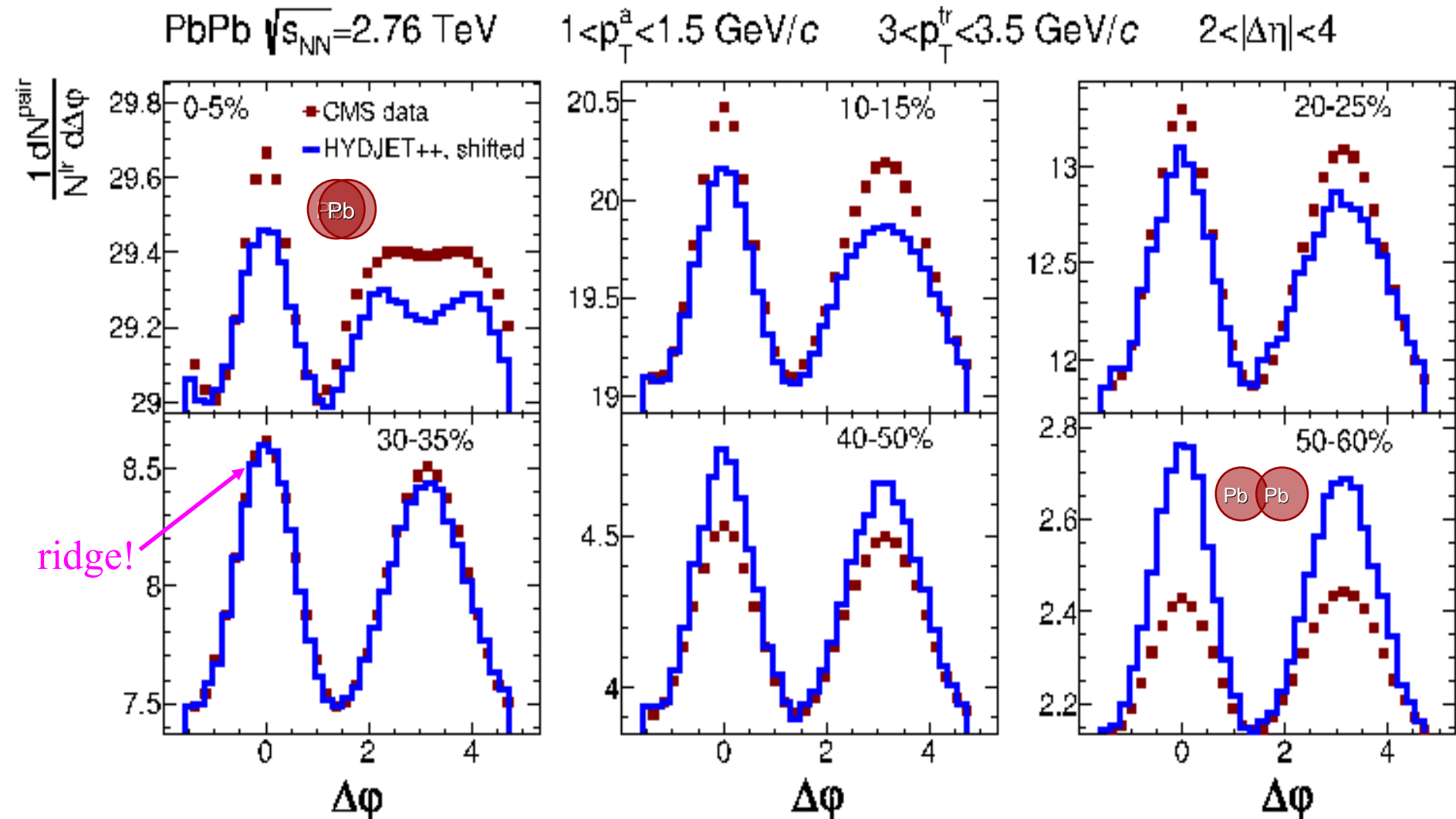
Elliptic and triangular flows of identified hadrons



Points: ALICE data ([JPG 38 \(2011\) 124047](#)); histograms: HYDJET++

HYDJET++ reproduces v_2 and v_3 for kaons and (anti-)protons, but rather underestimates the data for pions (stronger non-flow correlations in the data than in the model?)³

Dihadron angular correlations



Points: CMS data (*EPJC 72 (2012) 2012*); histograms: HYDJET++

Interplay of elliptic and triangular flows in HYDJET++ yields long-range 2-particle azimuthal correlations (*ridge effect*), but centrality dependence of the correlation strength seems to strong

1) Thermal charm production in HYDJET++ (soft component)

Thermal charmed hadrons J/ψ , D^0 , \bar{D}^0 , D^+ , D^- , D_s^+ , D_s^- , Λ_c^+ , Λ_c^- are generated within the statistical hadronization model

(*A.Andronic, P.Braun-Munzinger, K.Redlich, J.Stachel,*
Phys.Lett. B 571 (2003) 36; Nucl. Phys. A 789 (2007) 334)

$$N_D = \gamma_c N_D^{\text{th}} \left(I_1(\gamma_c N_D^{\text{th}}) / I_0(\gamma_c N_D^{\text{th}}) \right), \quad N_{J/\psi} = \gamma_c^2 N_{J/\psi}^{\text{th}}$$

γ_c - charm enhancement factor is obtained from the equation:

$$N_{cc} = 0.5 \gamma_c N_D^{\text{th}} \left(I_1(\gamma_c N_D^{\text{th}}) / I_0(\gamma_c N_D^{\text{th}}) \right) + \gamma_c^2 N_{J/\psi}^{\text{th}}$$

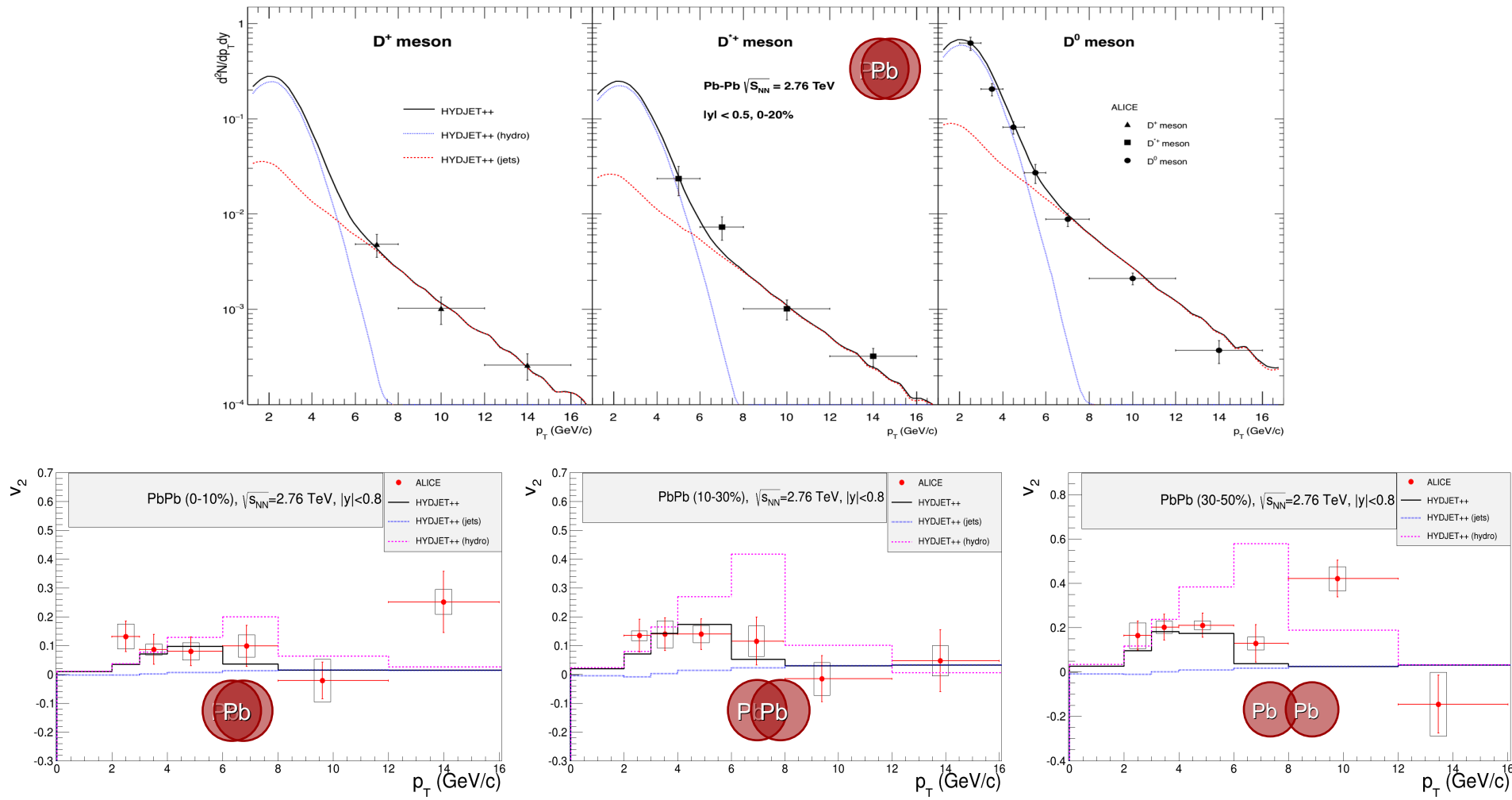
where number of c-quark pairs N_{cc} is calculated with PYTHIA

(the factor $K \sim 2$ is applied to take into account NLO pQCD corrections)
and multiplied by the number of NN sub-collisions for given centrality

2) Non-thermal charm production in HYDJET++ (hard component)

Non-thermal charmed hadrons are generated within
PYTHIA/PYQUEN taking into account medium-induced rescattering
and energy loss of heavy quarks (b, c)

P_T -spectra and elliptic flow of D^0 -mesons

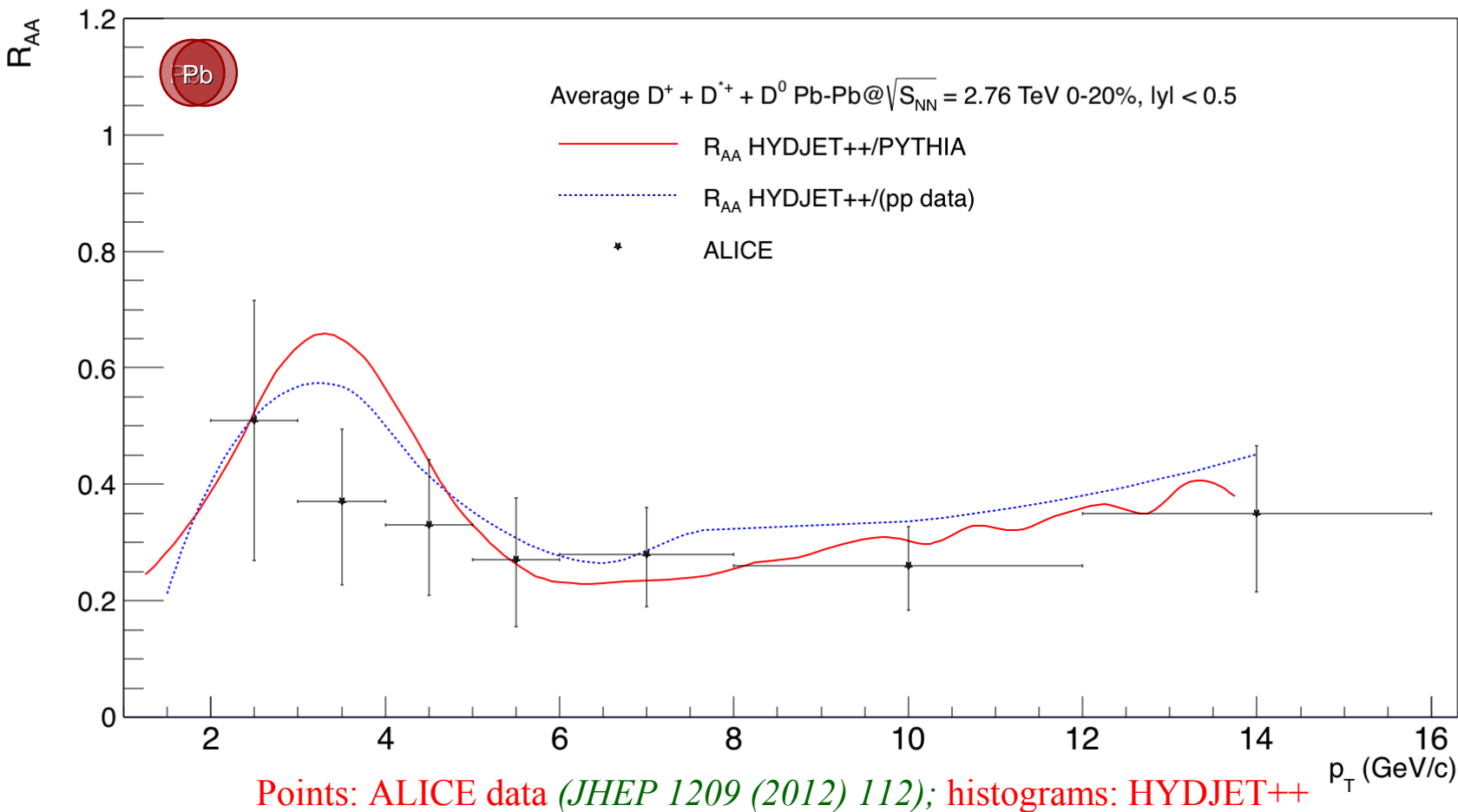


Points: ALICE data (*JHEP 1209 (2012) 112; PRC 90 (2014) 034904*); histograms: HYDJET++

HYDJET++ reproduces p_T -spectrum & $v_2(p_T)$ of D-mesons with the *same freeze-out parameters* as for inclusive hadrons \Rightarrow significant part of D-mesons (*thermal component*) is in the kinetic equilibrium with the medium; *non-thermal component* is important at high p_T

D mesons at LHC (nuclear modification factor R_{AA})

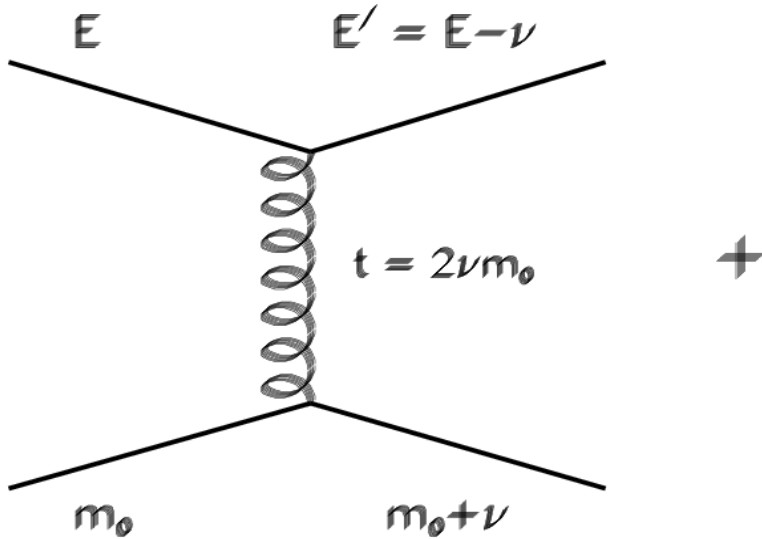
$$R_{AA} = \frac{\sigma_{pp}^{inel}}{\langle N_{coll} \rangle} \frac{d^2 N_{AA} / dp_T d\eta}{d^2 \sigma_{pp} / dp_T d\eta} \sim \begin{cases} \text{“QCD Medium”} \\ \text{“QCD Vacuum”} \end{cases} \quad \begin{cases} R_{AA} > 1: \text{enhancement} \\ R_{AA} = 1: \text{no medium effect} \\ R_{AA} < 1: \text{suppression} \end{cases}$$



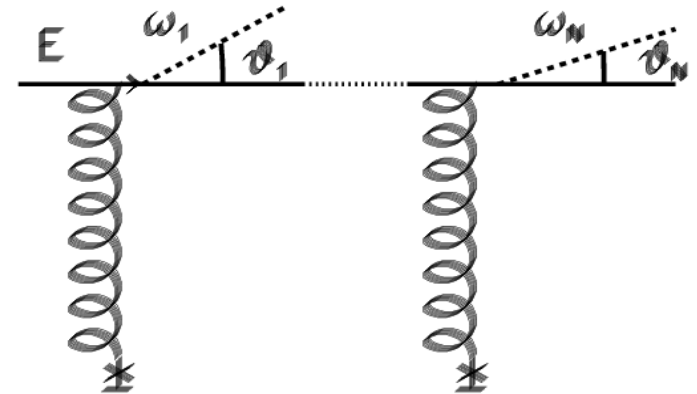
HYDJET++ reproduces $R_{AA}(p_T)$ of D-mesons up to very high $p_T \Rightarrow$ treatment of **heavy quark energy loss** in hard component of HYDJET++ (PYQUEN) seems quite successful

Medium-induced partonic rescattering and energy loss («jet quenching»)

Collisional loss
*(high momentum transfer
approximation)*



Radiative loss
*(BDMPS model,
coherent radiation)*



Angular structure of energy loss in PYQUEN

Radiative loss, three options (simple parametrizations) for angular distribution of in-medium emitted gluons:

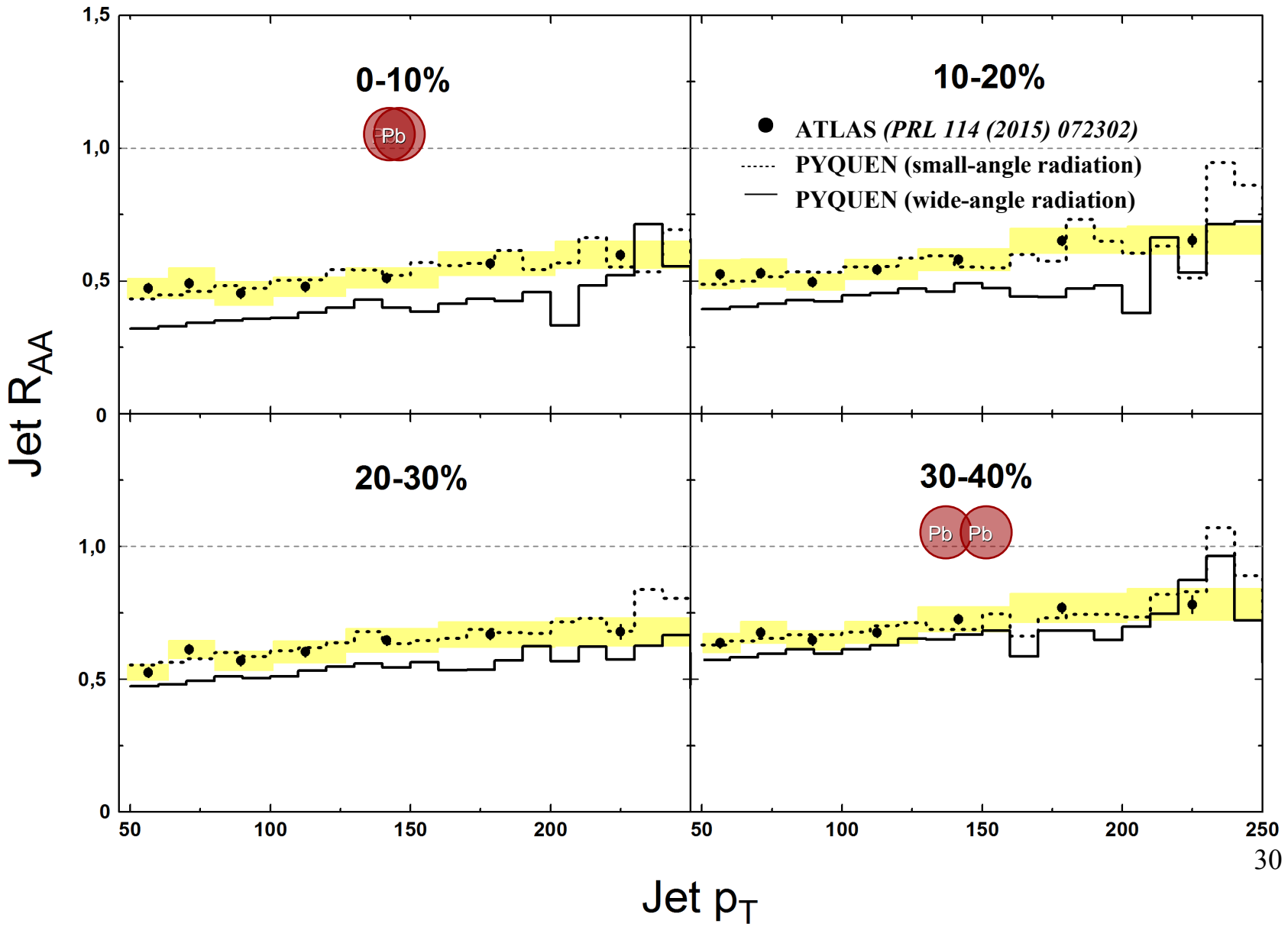
Collinear radiation $\theta=0$

Small-angular radiation $\frac{dN^g}{d\theta} \propto \sin \theta \exp\left(\frac{-(\theta-\theta_0)^2}{2\theta_0^2}\right), \quad \theta_0 \sim 5^\circ$

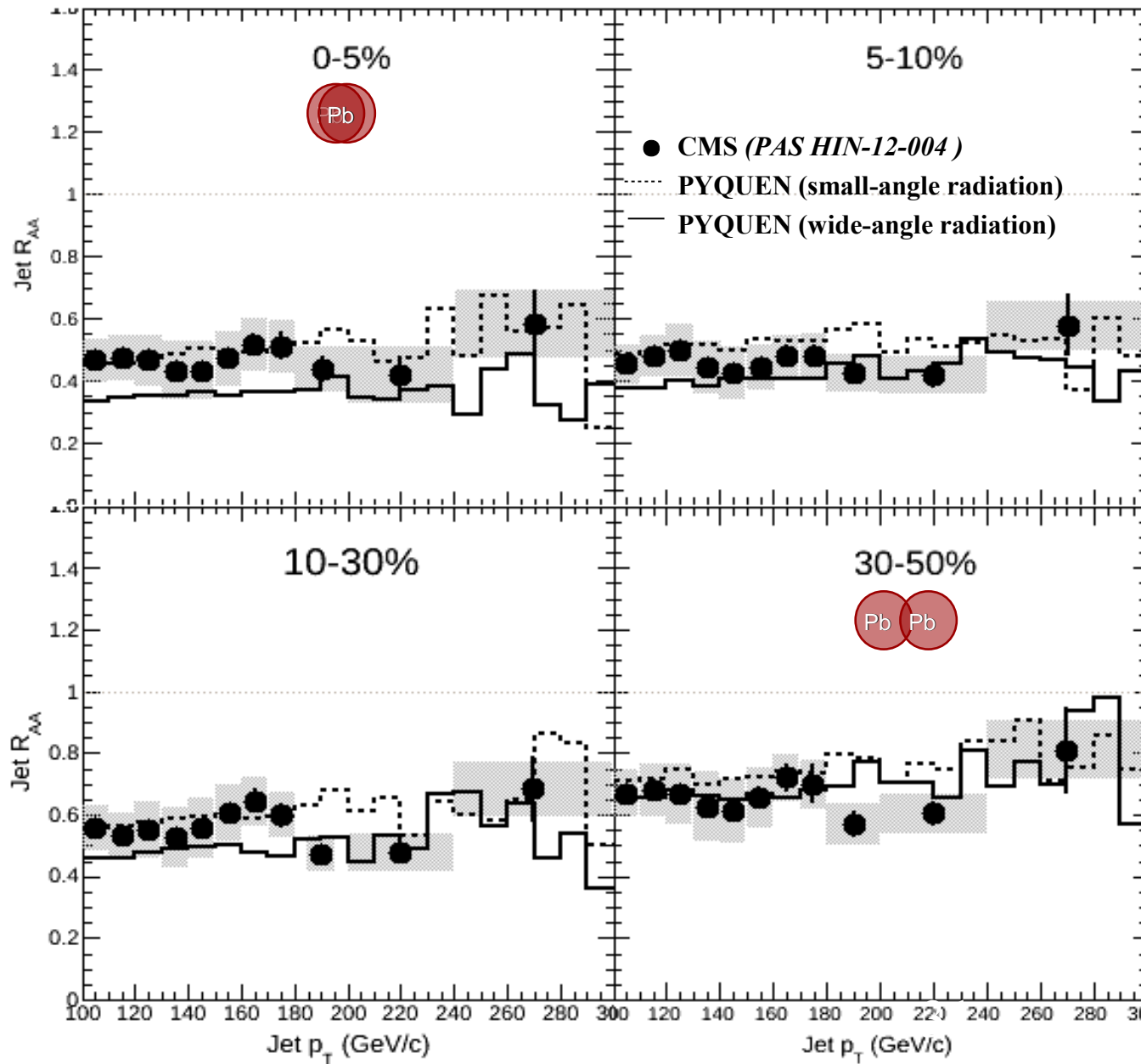
Wide-angular radiation $\frac{dN^g}{d\theta} \propto \frac{1}{\theta}$

Collisional loss always “out-of-cone” (energy is absorbed by medium)

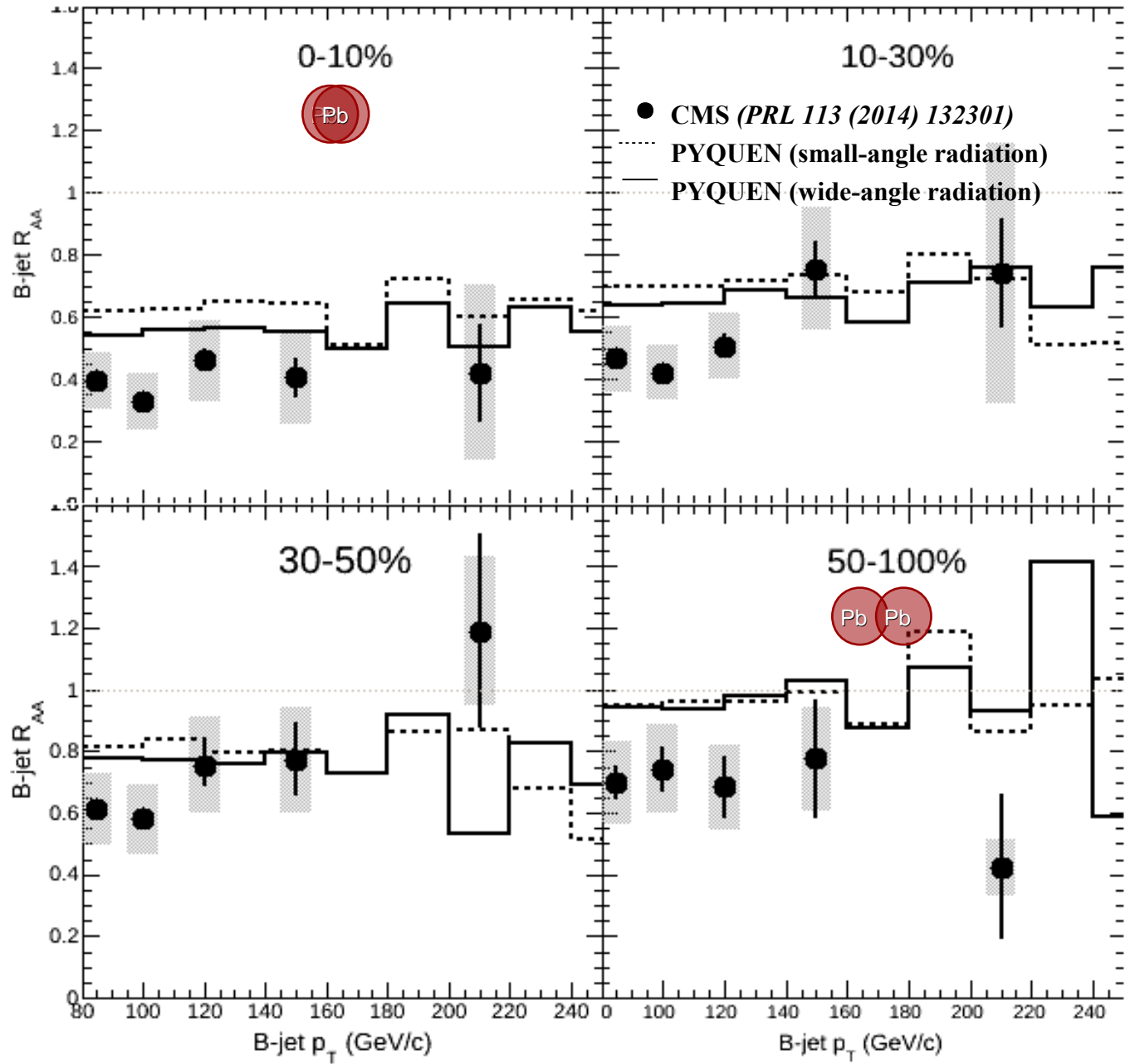
Suppression factor of inclusive jets



Suppression factor of inclusive jets

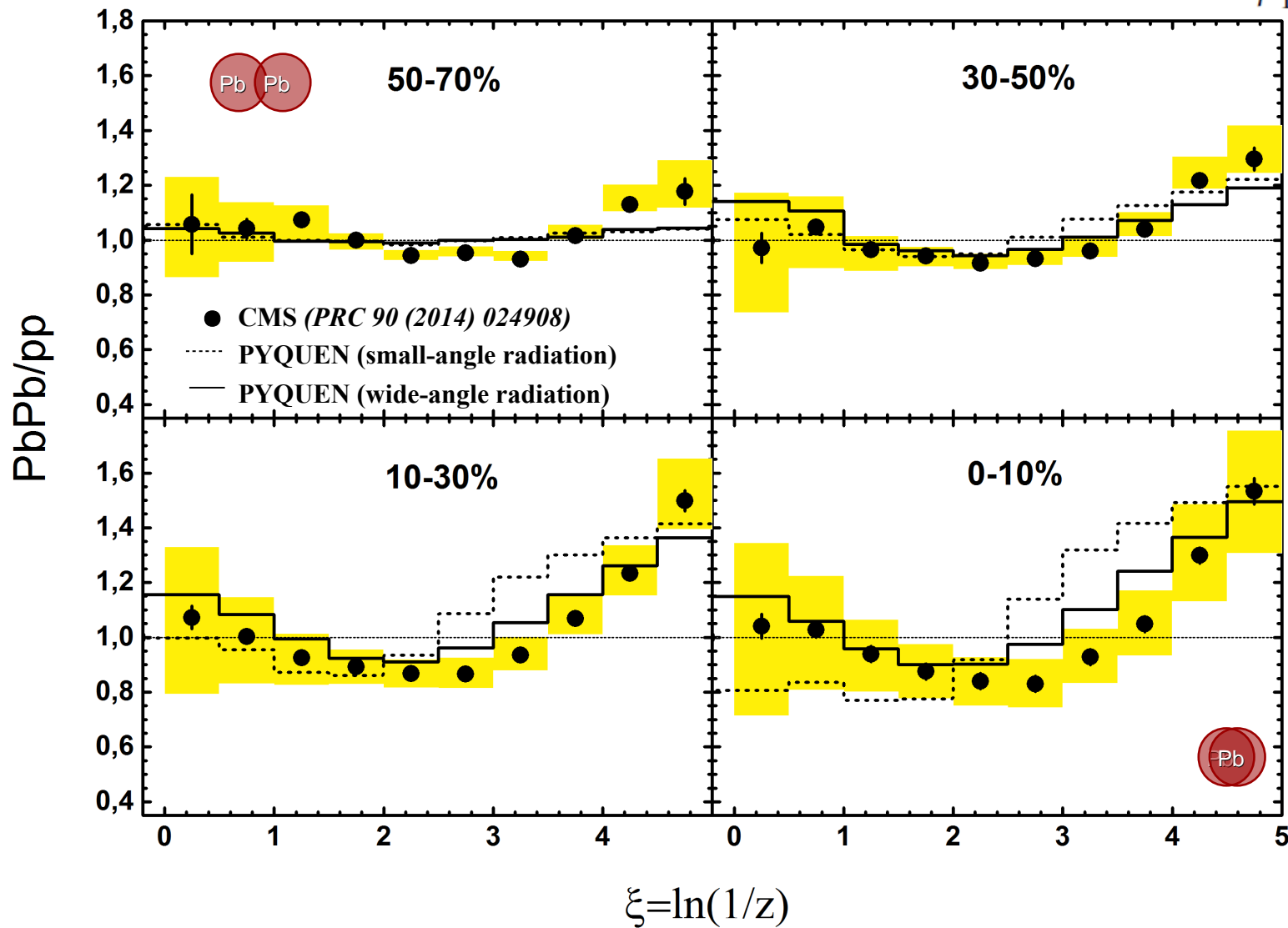


Suppression factor of b-jets



Jet fragmentation function

$$\xi = -\ln z = -\ln \frac{p_T^{track}}{p_T^{jet}}$$



$$\xi = \ln(1/z)$$

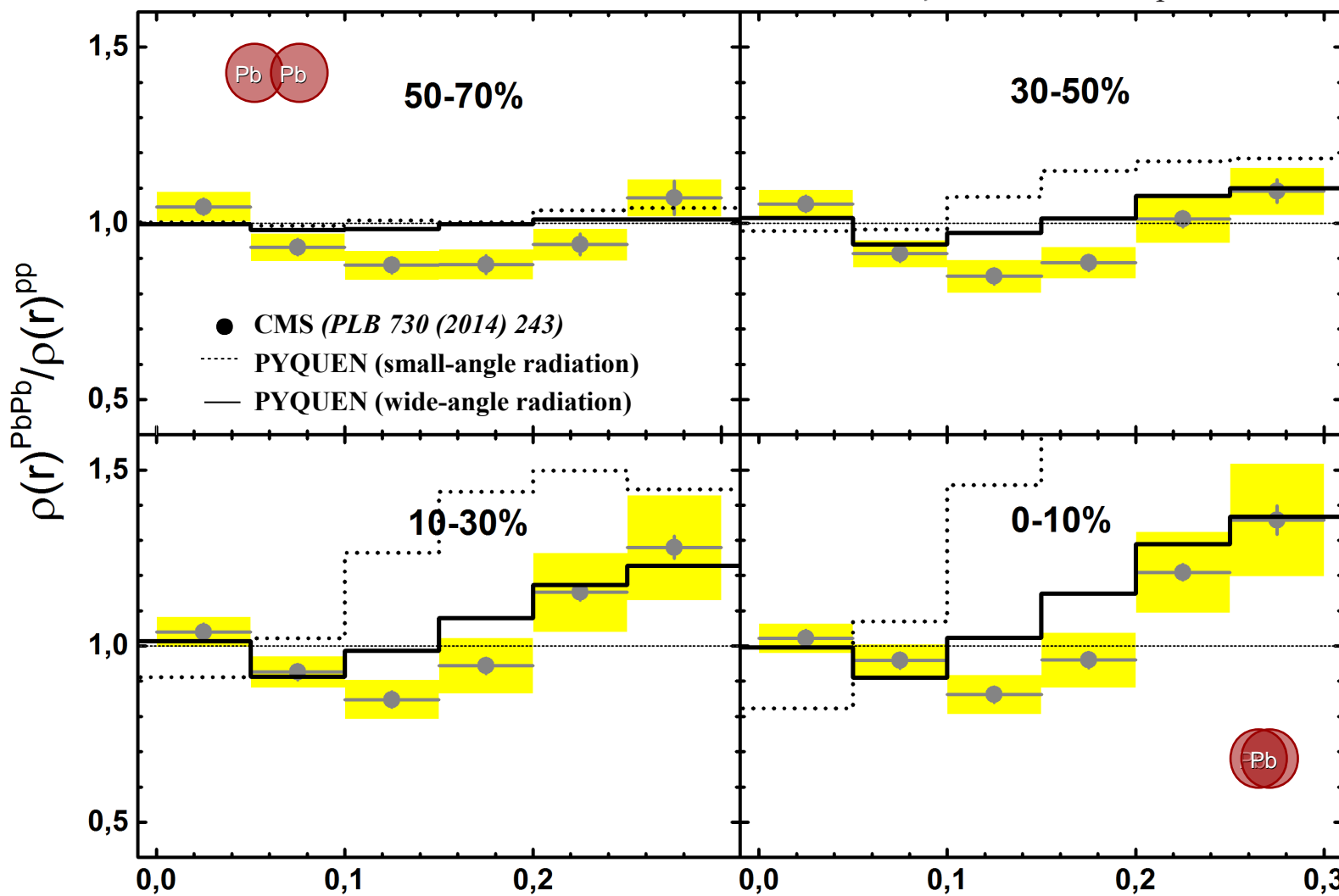
The modification of longitudinal jet profile ($E_T^{jet} > 100$ GeV, $R=0.3$):

excess at low p_T ; suppression at intermediate p_T ; high p_T is slightly enhanced.

Reproduced well by PYQUEN with wide-angle radiative + collisional partonic energy loss.

Jet shapes

$$\rho(r) \sim \frac{1}{\delta r} \frac{1}{N_{\text{jet}}} \sum_{\text{jets}} \frac{p_T(r - \delta r/2, r + \delta r/2)}{p_T^{\text{jet}}}$$



The modification of *radial jet profile* ($E_T^{\text{jet}} > 100 \text{ GeV}, R=0.3$):

excess at large radii; suppression at intermediate radii; core is unchanged.

Reproduced well by PYQUEN with *wide-angle radiative + collisional partonic energy loss*.

Main publications (2011-2015)

- [1] I.P. Lokhtin, A.V. Belyaev, A.M. Snigirev, “Jet quenching pattern at LHC in PYQUEN model”, *Eur. Phys. J. C* 71 (2011) 1650
- [2] I.P. Lokhtin, A.V. Belyaev, L.V. Malinina, S.V. Petrushanko, E.P. Rogochaya, A.M. Snigirev, “Hadron spectra, flow and correlations in PbPb collisions at the LHC: interplay between soft and hard physics”, *Eur. Phys. J. C* 72 (2012) 2045
- [3] L.V. Bravina, B.H. Brusheim Johansson, G.Kh. Eyyubova, V.L. Korotkikh, I.P. Lokhtin, L.V. Malinina, S.V. Petrushanko, A.M. Snigirev, E.E. Zabrodin. “Hexagonal flow v_6 as a superposition of elliptic v_2 and triangular v_3 flows”, *Phys. Rev. C* 89 (2014) 024909
- [4] L.V. Bravina, B.H. Brusheim Johansson, G.Kh. Eyyubova, V.L. Korotkikh, I.P. Lokhtin, L.V. Malinina, S.V. Petrushanko, A.M. Snigirev, E.E. Zabrodin. “Higher harmonics of azimuthal anisotropy in relativistic heavy ion collisions in HYDJET++ model”, *Eur. Phys. J. C* 74 (2014) 2807
- [5] I.P. Lokhtin, A.A. Alkin, A.M. Snigirev, “On jet structure in heavy ion collisions”, *arXiv 1410.0147, submitted to Eur. Phys. J. C*
- [6] G. Eyyubova, V.L. Korotkikh, I.P. Lokhtin, S.V. Petrushanko, A.M. Snigirev, L.V. Bravina, E.E. Zabrodin, “Angular dihadron correlations as interplay of elliptic and triangular flows”, *Phys. Rev. C* 91 (2015) 064907
- [7] I.P. Lokhtin, A.V. Belyaev, G.Kh. Eyyubova, G. Ponimatkina, E. Pronina, “Thermal and non-thermal charmed meson production in heavy ion collisions at the LHC”, *in preparation*
- [8] V.L. Korotkikh, I.P. Lokhtin, L.V. Malinina, E.N. Nazarova, S.V. Petrushanko, A.M. Snigirev, E.S. Fotina, “Anisotropic flow fluctuations in hydro-inspired freeze-out model for relativistic heavy ion collisions”, *in preparation*

SUMMARY

SUMMARY

Two-component model of relativistic heavy ion collisions HYDJET++ reproduces basic physical observables measured in PbPb collisions at the LHC:

- multiplicity and momentum spectra of inclusive and identified hadrons
- anisotropic flow of inclusive and identified hadrons (including odd and higher harmonics)
- two-particle angular correlations of inclusive hadrons (including “ridge”)
- momentum spectra and elliptic flow of D-mesons
- femtoscopic correlation radii of pion pairs
- transverse momentum imbalance in dijet production
- suppression of hard hadron and jet yields (including b-jets)
- modification of internal jet structure (longitudinal and radial profiles)

SUMMARY

Two-component model of relativistic heavy ion collisions HYDJET++ reproduces basic physical observables measured in PbPb collisions at the LHC:

- multiplicity and momentum spectra of inclusive and identified hadrons
- anisotropic flow of inclusive and identified hadrons (including odd and higher harmonics)
- two-particle angular correlations of inclusive hadrons (including “ridge”)
- momentum spectra and elliptic flow of D-mesons
- femtoscopic correlation radii of pion pairs
- transverse momentum imbalance in dijet production
- suppression of hard hadron and jet yields (including b-jets)
- modification of internal jet structure (longitudinal and radial profiles)

The pattern of multi-hadron and jet production in most central PbPb collisions at the LHC agrees with the formation of hot strongly-interacting matter with hydrodynamical properties (“quark-gluon fluid”), which absorbs energetic quarks and gluons due to their multiple scattering and wide-angle radiative and collisional medium-induced energy loss.

SUMMARY

Two-component model of relativistic heavy ion collisions HYDJET++ reproduces basic physical observables measured in PbPb collisions at the LHC:

- multiplicity and momentum spectra of inclusive and identified hadrons
- anisotropic flow of inclusive and identified hadrons (including odd and higher harmonics)
- two-particle angular correlations of inclusive hadrons (including “ridge”)
- momentum spectra and elliptic flow of D-mesons
- femtoscopic correlation radii of pion pairs
- transverse momentum imbalance in dijet production
- suppression of hard hadron and jet yields (including b-jets)
- modification of internal jet structure (longitudinal and radial profiles)

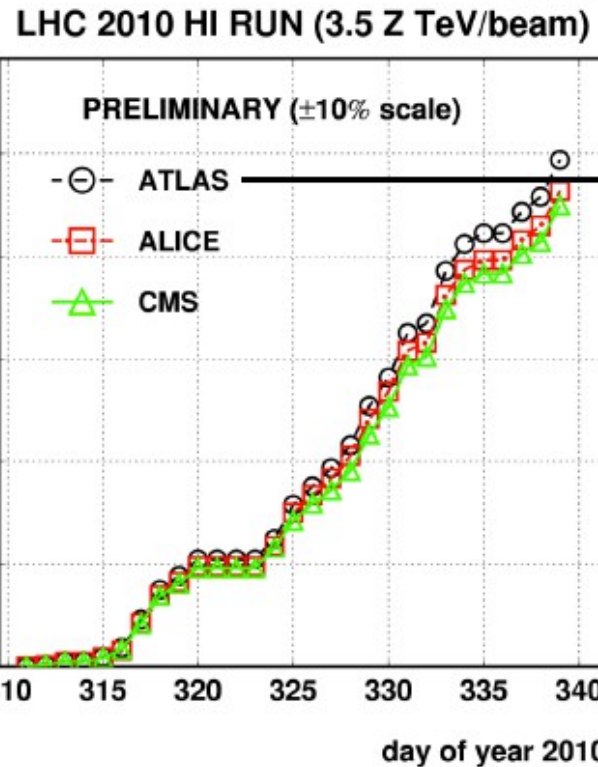
The pattern of multi-hadron and jet production in most central PbPb collisions at the LHC agrees with the formation of hot strongly-interacting matter with hydrodynamical properties (“quark-gluon fluid”), which absorbs energetic quarks and gluons due to their multiple scattering and wide-angle radiative and collisional medium-induced energy loss.

Works in progress and near plans related to phenomenological analysis of LHC heavy ion data and the model improvements:

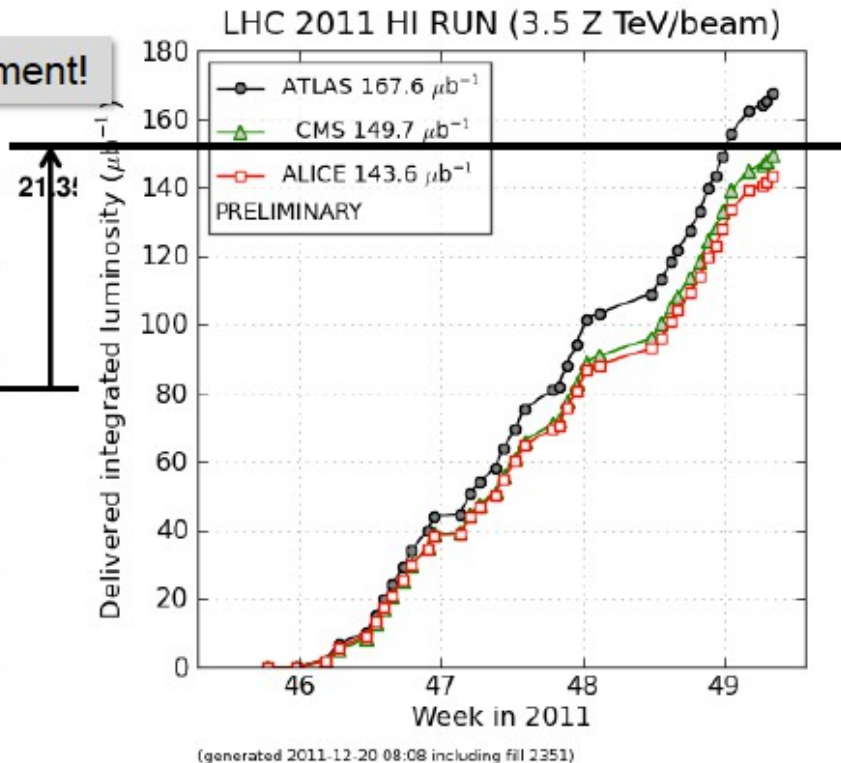
- event-by-event fluctuations of anisotropic flow
- azimuthal dependence of femtoscopic correlation radii
- momentum spectra and elliptic flow of J/ ψ -mesons
- ...

BACKUP SLIDES

delivered integrated luminosity (μb^{-1})



factor 16 improvement!



Period	Species	Energy	Lumi
Dec. 2010	Pb+Pb	2.76 TeV	7 μb^{-1}
Dec. 2011	Pb+Pb	2.76 TeV	150 μb^{-1}
Mar. 2011	p+p	2.76 TeV	230 nb $^{-1}$
Jan. 2013	p+Pb	5.02 TeV	35 nb $^{-1}$
Fev. 2013	p+p	2.76 TeV	5.4 $^{+1}_{-1}$ pb $^{-1}$

PYQUEN: physics frames

General kinetic integral equation:

$$\Delta E(L, E) = \int_0^L dx \frac{dP}{dx}(x) \lambda(x) \frac{dE}{dx}(x, E), \quad \frac{dP}{dx}(x) = \frac{1}{\lambda(x)} \exp(-x/\lambda(x))$$

1. Collisional loss and elastic scattering cross section:

$$\frac{dE}{dx} = \frac{1}{4T\lambda\sigma} \int_{\mu_D^2}^{t_{max}} dt \frac{d\sigma}{dt} t, \quad \frac{d\sigma}{dt} \simeq C \frac{2\pi\alpha_s^2(t)}{t^2}, \quad \alpha_s = \frac{12\pi}{(33-2N_f)\ln(t/\Lambda_{QCD}^2)}, \quad C = 9/4(gg), 1(gq), 4/9(qq)$$

2. Radiative loss (BDMPS):

$$\frac{dE}{dx}(m_q=0) = \frac{2\alpha_s C_F}{\pi\tau_L} \int_{E_{LPM} \sim \lambda_g \mu_D^2}^E d\omega \left[1 - y + \frac{y^2}{2} \right] \ln |\cos(\omega_1 \tau_1)|, \quad \omega_1 = \sqrt{i \left(1 - y + \frac{C_F}{3} y^2 \right) \bar{k} \ln \frac{16}{\bar{k}}}, \quad \bar{k} = \frac{\mu_D^2 \lambda_g}{\omega(1-y)}, \quad \tau_1 = \frac{\tau_L}{2\lambda_g}, \quad y = \frac{\omega}{E}, \quad C_F = \frac{4}{3}$$

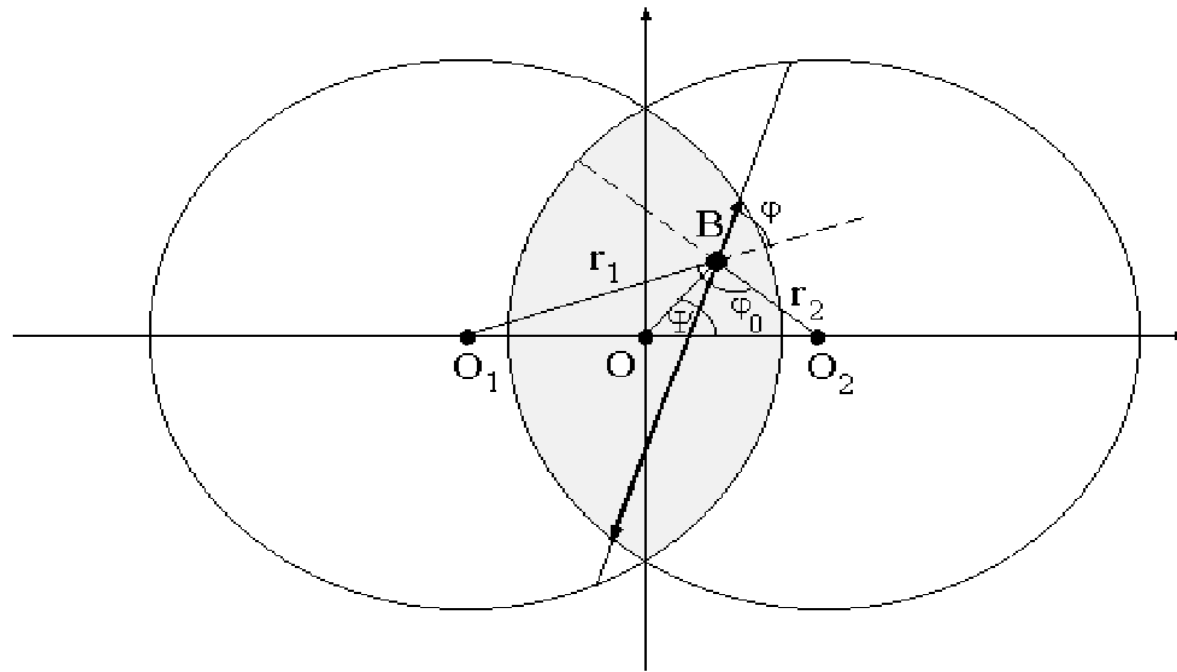
“dead cone” approximation for massive quarks:

$$\frac{dE}{dx}(m_q \neq 0) = \frac{1}{(1 + (l\omega)^{3/2})^2} \frac{dE}{dx}(m_q=0), \quad l = \left(\frac{\lambda}{\mu_D^2} \right)^{1/3} \left(\frac{m_q}{E} \right)^{4/3}$$

Nuclear geometry and QGP evolution

impact parameter $b \equiv |O_1 O_2|$ - transverse distance between nucleus centers

$$\varepsilon(r_1, r_2) \propto T_A(r_1) * T_A(r_2) \quad (T_A(b) - \text{nuclear thickness function})$$



Space-time evolution of QGP, created in region of initial overlapping of colliding nuclei, is described by Lorenz-invariant Bjorken's hydrodynamics *J.D. Bjorken, PRD 27 (1983) 140*

Monte-Carlo simulation of parton rescattering and energy loss in PYQUEN

- Distribution over jet production vertex $V(r \cos\psi, r \sin\psi)$ at im.p. b

$$\frac{dN}{d\psi dr}(b) = \frac{T_A(r_1)T_A(r_2)}{\int_0^{2\pi} d\psi \int_0^{r_{max}} r dr T_A(r_1)T_A(r_2)}$$

- Transverse distance between parton scatterings $l_i = (\tau_{i+1} - \tau_i) E/p_T$

$$\frac{dP}{dl_i} = \lambda^{-1}(\tau_{i+1}) \exp\left(-\int_0^{l_i} \lambda^{-1}(\tau_i + s) ds\right), \quad \lambda^{-1} = \sigma \rho$$

- Radiative and collisional energy loss per scattering

$$\Delta E_{tot,i} = \Delta E_{rad,i} + \Delta E_{col,i}$$

- Transverse momentum kick per scattering

$$\Delta k_{t,i}^2 = \left(E - \frac{t_i}{2m_{0i}}\right)^2 - \left(p - \frac{E}{p} \frac{t_i}{2m_{0i}} - \frac{t_i}{2p}\right)^2 - m_q^2$$

HYDJET(soft): physics frames & simulation procedure

The final hadron spectrum are given by the superposition of thermal distribution and collective flow assuming Bjorken's scaling.

1. Thermal distribution of produced hadron in rest frame of fluid element

$$f(E_0) \propto E_0 \sqrt{E_0^2 - m^2} \exp(-E_0/T_f), \quad -1 < \cos \theta_0 < 1, \quad 0 < \phi_0 < 2\pi$$

2. Space position r and local 4-velocity u_μ

$$f(r) = 2r/R_f^2(R_A, b, \Phi) (0 < r < R_f), \quad f(\eta) \propto e^{-\frac{-(\eta - Y_L^{max})^2}{2(Y_L^{max})^2}}, \quad 0 < \Phi < 2\pi$$
$$u_r = \sinh Y_T^{max} \cdot r / \sqrt{R_{eff}(R_A, b) \cdot R_A}, \quad u_t = \sqrt{1 + u_r^2} \cosh \eta, \quad u_z = \sqrt{1 + u_r^2} \sinh \eta$$

3. Boost of hadron 4-momentum p_μ in c.m. frame of the event

$$p_x = p_0 \sin \theta_0 \cos \phi_0 + u_r \cos \Phi [E_0 + (u^i p_0^i)/(u_t + 1)],$$

$$p_y = p_0 \sin \theta_0 \sin \phi_0 + u_r \sin \Phi [E_0 + (u^i p_0^i)/(u_t + 1)],$$

$$p_z = p_0 \cos \theta_0 + u_z [E_0 + (u^i p_0^i)/(u_t + 1)],$$

$$E = E_0 u_t + (u^i p_0^i), \quad (u^i p_0^i) = u_r p_0 \sin \theta_0 \cos(\Phi - \phi_0) + u_z p_0 \cos \theta_0$$

Monte-Carlo simulation of hard component (including nuclear shadowing) in HYDJET/HYDJET++

- Calculating the number of hard NN sub-collisions N_{jet} (b , Pt_{min} , \sqrt{s}) with $Pt > Pt_{min}$ around its mean value according to the binomial distribution.
- Selecting the type (for each of N_{jet}) of hard NN sub-collisions (pp, np or nn) depending on number of protons (Z) and neutrons ($A-Z$) in nucleus A according to the formula: $Z=A/(1.98+0.015A^{2/3})$.
- Generating the hard component by calling PYQUEN n_{jet} times.
- Correcting the PDF in nucleus by the accepting/rejecting procedure for each of N_{jet} hard NN sub-collisions: comparision of random number generated uniformly in the interval $[0,1]$ with shadowing factor $S(r_1, r_2, x_1, x_2, Q^2) \leq 1$ taken from the adapted impact parameter dependent parameterization based on Glauber-Gribov theory (*K.Tywoniuk et al., Phys. Lett. B 657 (2007) 170*).

HYDJET: model parameters

Minimal external input

A - beam and target nucleus atomic weight;

energy - c.m.s. energy per nucleon pair;

ifb, bmin, bmax, bfix – parameters to fix event centrality selection;

nh- total mean multiplicity of primary hadrons for soft component (PbPb, $b=0$);

(multiplicity for other centralities and atomic weights is calculated automatically).

Parameter can be varied by user

ytfl - maximum transverse collective rapidity, controls slope of low-pt spectra;

ylfl - maximum longitudinal collective rapidity, controls width of η -spectra;

Tf – hadron thermal freeze-out temperature;

fpart - fraction of soft multiplicity proportional to # of participants ($fpart(D)=1$);

sigin – inelastic NN cross-section (calculated by PYTHIA by default);

ptmin - minimal transverse momentum of “non-thermalized” initial parton-parton scatterings (=ckin(3) in PYTHIA; other PYTHIA parameters also can be varied);

T0, tau0, nf, ienglu, ianglu – PYQUEN parameters;

nhsel - flag to switch on/off jet production and jet quenching;

ishad - flag to switch on/off nuclear shadowing.

Internal sets for soft component

poison multiplicity distribution; thermal particle ratios.

HYDJET++ (soft): main physics assumptions

A hydrodynamic expansion of the fireball is supposed ends by a sudden system breakup at given T and chemical potentials. Momentum distribution of produced hadrons keeps the thermal character of the equilibrium distribution.

Cooper-Frye formula: $p^0 \frac{d^3 N_i}{d^3 p} = \int_{\sigma(x)} d^3 \sigma_\mu(x) p^\mu f_i^{eq}(p^\nu u_\mu(x); T, \mu_i)$

- HYDJET++ avoids straightforward 6-dimensional integration by using the special simulation procedure (like HYDJET): momentum generation in the rest frame of fluid element, then Lorentz transformation in the global frame → uniform weights → effective von-Neumann rejection-acceptance procedure.

Freeze-out surface parameterizations

1. The Bjorken model with hypersurface

$$\tau = (t^2 - z^2)^{1/2} = const$$

2. Linear transverse flow rapidity profile

$$\rho_u = \frac{r}{R} \rho_u^{\max}$$

3. The total effective volume for particle production at

- $V_{eff} = \int_{\sigma(x)} d^3 \sigma_\mu(x) u^\mu(x) = \tau \int_0^R \gamma_r r dr \int_0^{2\pi} d\phi \int_{\eta_{min}}^{\eta_{\max}} d\eta = 2\pi \tau \Delta \eta \left(\frac{R}{\rho_u^{\max}} \right)^2 (\rho_u^{\max} \sinh \rho_u^{\max} - \cosh \rho_u^{\max} + 1)$

HYDJET++ (soft): hadron multiplicities

1. The hadronic matter created in heavy-ion collisions is considered as a hydrodynamically expanding fireball with EOS of an ideal hadron gas.
2. “Concept of effective volume” $T=\text{const}$ and $\mu=\text{const}$: the total yield of particle species is $N_i = \rho_i(T, \mu_i) V_{\text{eff}}$
3. Chemical freeze-out : $T, \mu_i = \mu_B B_i + \mu_S S_i + \mu_c C_i + \mu_Q Q_i$; T, μ_B –can be fixed by particle ratios, or by phenomenological formulas

$$T(\mu_B) = a - b\mu_B - c\mu_B^4; \mu_B(\sqrt{s_{NN}}) = \frac{d}{1 + e\sqrt{s_{NN}}}$$

4. Chemical freeze-out: all macroscopic characteristics of particle system are determined via a set of equilibrium distribution functions in the fluid element rest frame:

$$f_i^{eq}(p^{0*}; T, \mu_i) = \frac{1}{(2\pi)^3} \frac{g_i}{\exp([p^{0*} - \mu_i]/T) \pm 1}$$

$$\rho_i^{eq}(T, \mu_i) = \int_0^\infty d^3 \vec{p}^* f_i^{eq}(p^{0*}; T(x^*), \mu(x^*)_i) = 4\pi \int_0^\infty dp^* p^{*2} f_i^{eq}(p^{0*}; T, \mu_i)$$

HYDJET++ (soft): thermal and chemical freeze-outs

1. The particle densities at the chemical freeze-out stage are too high to consider particles as free streaming and to associate this stage with the **thermal freeze-out**
2. Within the concept of chemically frozen evolution, assumption of the conservation of the particle number ratios from the chemical to thermal freeze-out :

$$\frac{\rho_i^{eq}(T^{ch}, \mu_i^{ch})}{\rho_\pi^{eq}(T^{ch}, \mu_\pi^{ch})} = \frac{\rho_i^{eq}(T^{th}, \mu_i^{th})}{\rho_\pi^{eq}(T^{th}, \mu_\pi^{th})}$$

3. The absolute values $\rho_i^{eq}(T^{th}, \mu_i^{th})$ are determined by the choice of the **free parameter of the model: effective pion chemical potential** $\mu_\pi^{eff,th}$ at T^{th}
Assuming for the other particles (heavier than pions) the Boltzmann approximation :

$$\mu_i^{th} = T^{th} \ln \left(\frac{\rho_i^{eq}(T^{ch}, \mu_i^{ch})}{\rho_i^{eq}(T^{th}, \mu_i = 0)} \frac{\rho_\pi^{eq}(T^{th}, \mu_\pi^{eff,th})}{\rho_\pi^{eq}(T^{ch}, \mu_\pi^{ch})} \right)$$

Particle momentum spectra are generated on the **thermal freeze-out hypersurface**, the hadronic composition at this stage is defined by the parameters of the system at chemical freeze-out

HYDJET++ (soft): input parameters

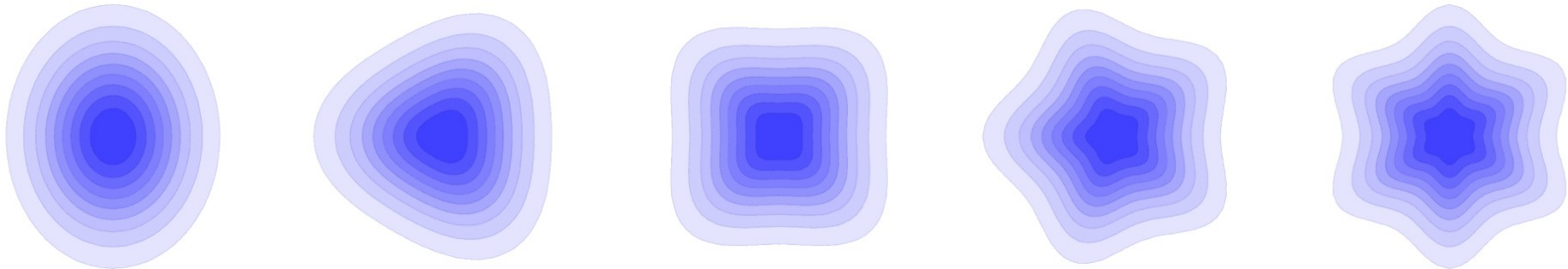
- 1-5. Thermodynamic parameters at chemical freeze-out: T^{ch} , $\{\mu_B, \mu_s, \mu_C, \mu_Q\}$ (option to calculate T^{ch} , μ_B and μ_s using phenomenological parameterization $\mu_B(\sqrt{s})$, $T^{ch}(\mu_B)$ is foreseen).
- 6-7. Strangeness suppression factor $\gamma_s \leq 1$ and charm enhancement factor $\gamma_c \geq 1$ (options to use phenomenological parameterization $\gamma_s(T^{ch}, \mu_B)$ and to calculate γ_c are foreseen).
- 8-9. Thermodynamical parameters at thermal freeze-out: T^{th} , and μ_π - effective chemical potential of positively charged pions.
- 10-12. Volume parameters at thermal freeze-out: proper time τ_f , its standard deviation (emission duration) $\Delta\tau_f$, maximal transverse radius R_f .
13. Maximal transverse flow rapidity at thermal freeze-out ρ_u^{\max} .
14. Maximal longitudinal flow rapidity at thermal freeze-out η^{\max} .
15. Flow anisotropy parameter: $\delta(b) \rightarrow u^\mu = u^\mu(\delta(b), \varphi)$
16. Coordinate anisotropy: $\varepsilon(b) \rightarrow R_f(b) = R_f(0)[V_{eff}(\varepsilon(0), \delta(0))/V_{eff}(\varepsilon(b), \delta(b))]^{1/2}[N_{part}(b)/N_{part}(0)]^{1/3}$

For impact parameter range b_{min} - b_{max} :

$$V_{eff}(b) = V_{eff}(0)N_{part}(b)/N_{part}(0), \quad \tau_f(b) = \tau_f(0)[N_{part}(b)/N_{part}(0)]^{1/3}$$

Higher harmonic flow

Non-zero high Fourier coefficients carry information about the details of the space-time evolution of QCD-matter and initial state fluctuations.



$n = 2$

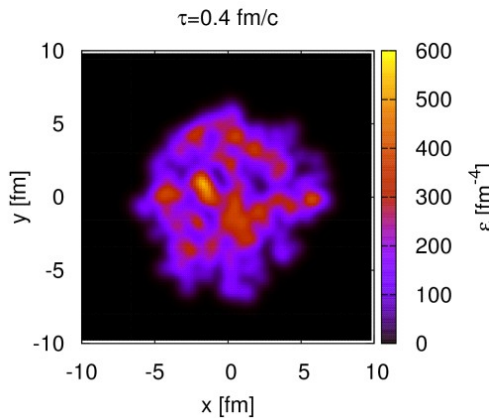
$n = 3$

$n = 4$

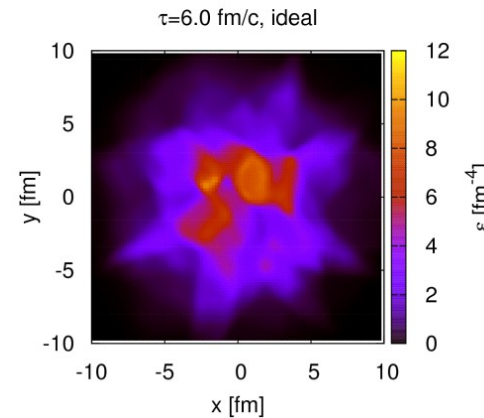
$n = 5$

$n = 6$

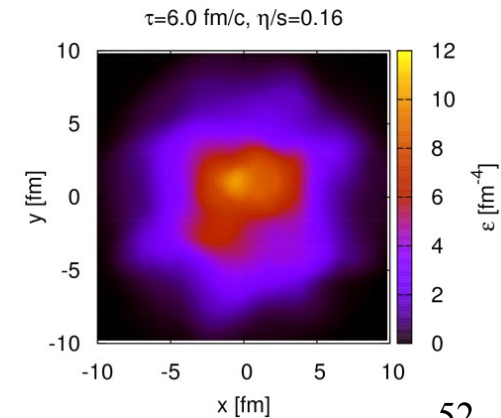
initial



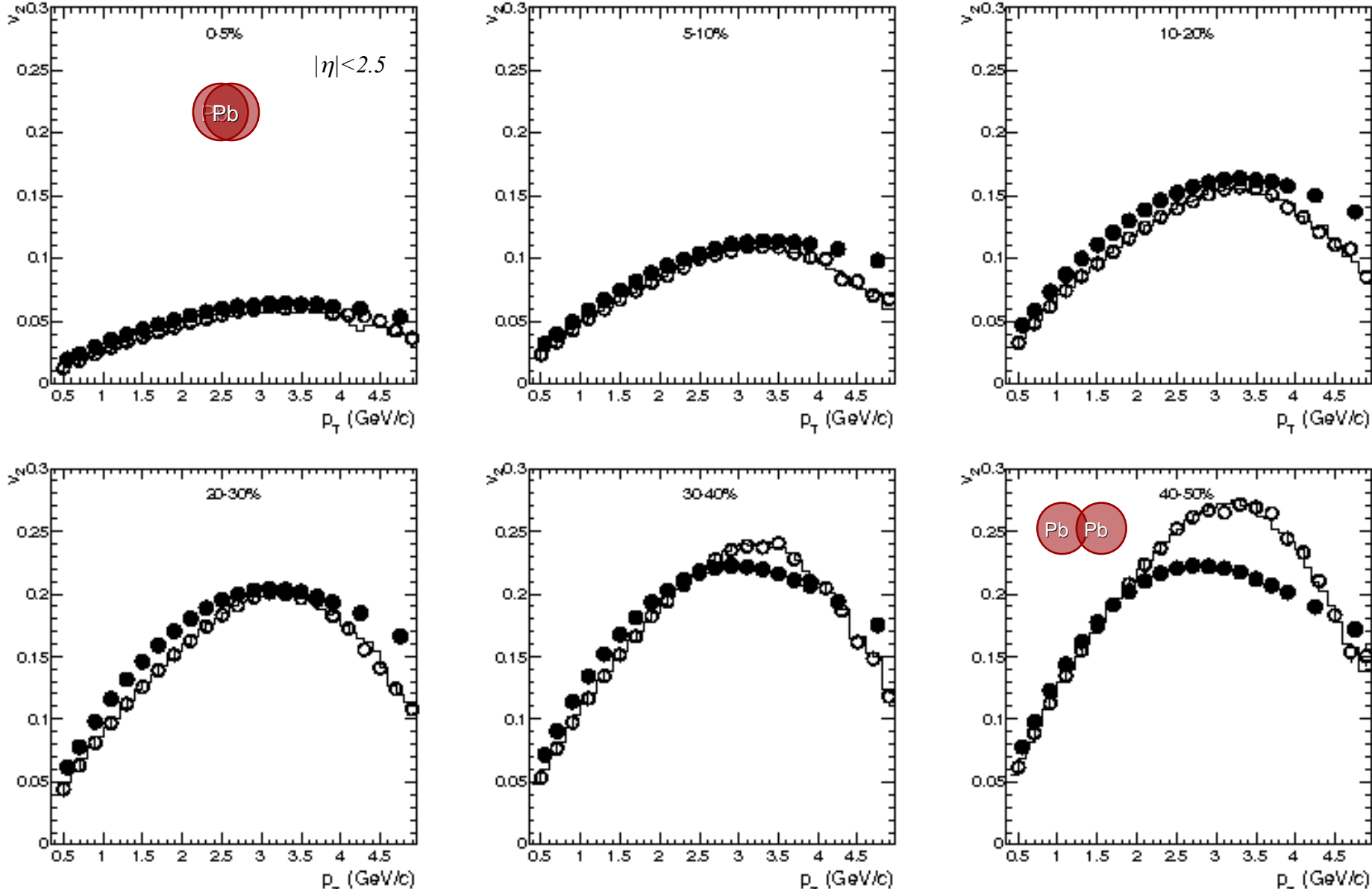
ideal



viscous



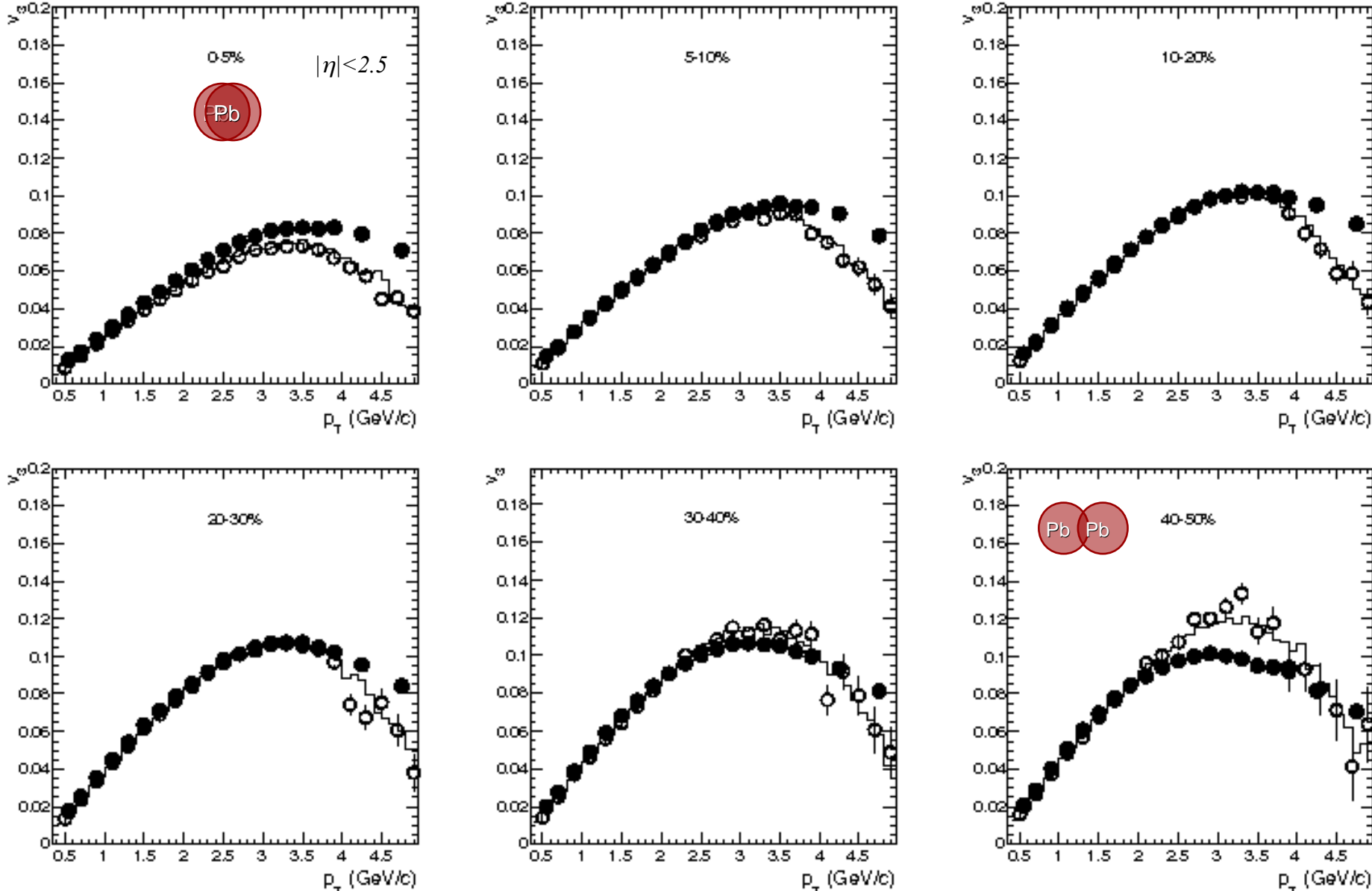
Elliptic flow of inclusive charged hadrons



Closed circles: ATLAS data $v_2\{\text{EP}\}$ (*PRC 86 (2012) 014907*);

histograms and open circles: HYDJET++ (“true” $v_2(\psi_2)$ & $v_2\{\text{EP}\}$)

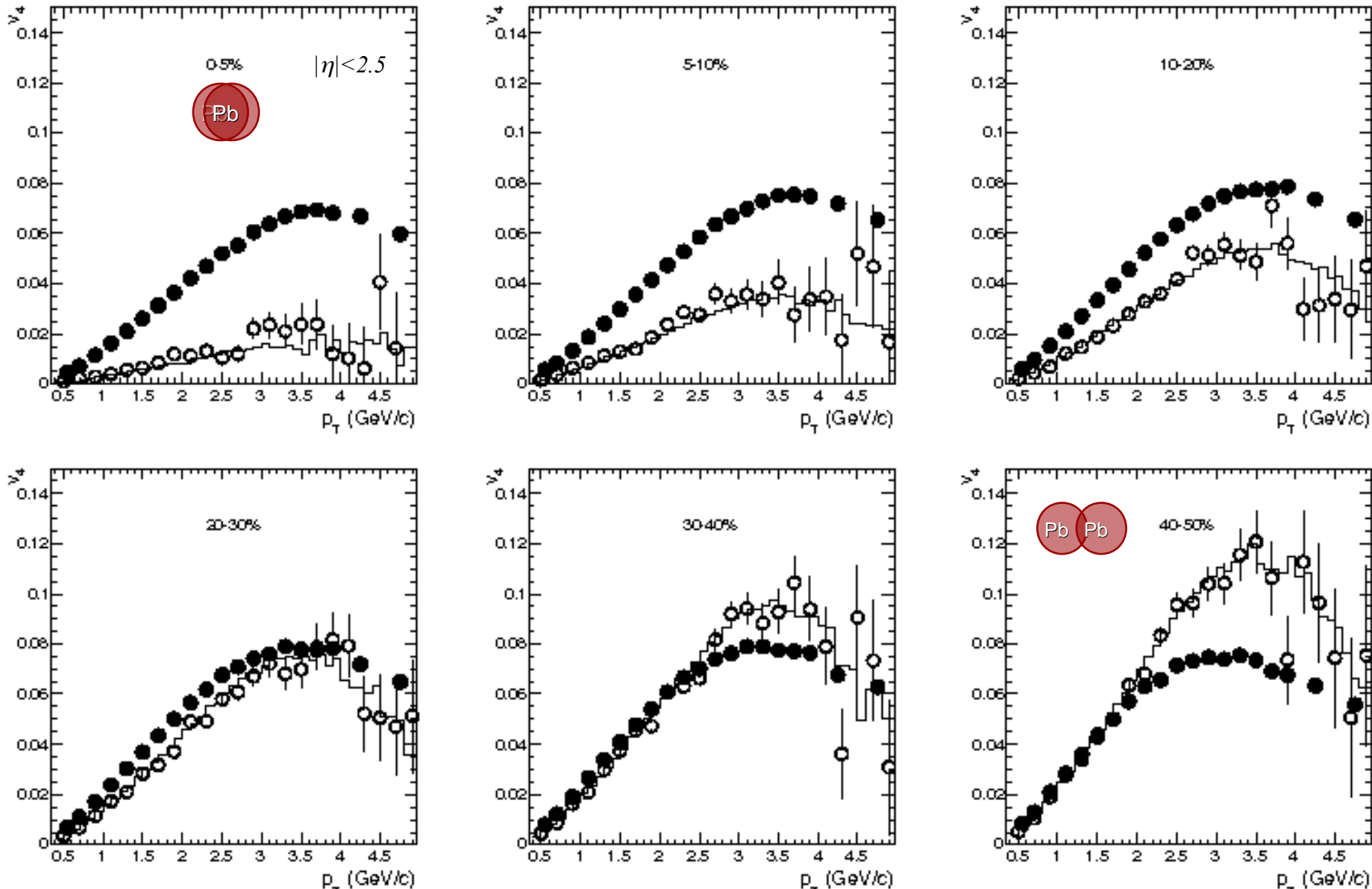
Triangular flow of inclusive charged hadrons



Closed circles: ATLAS data $v_3\{\text{EP}\}$ (*PRC 86 (2012) 014907*);

histograms and open circles: HYDJET++ (“true” $v_3(\psi_3)$ & $v_3\{\text{EP}\}$)

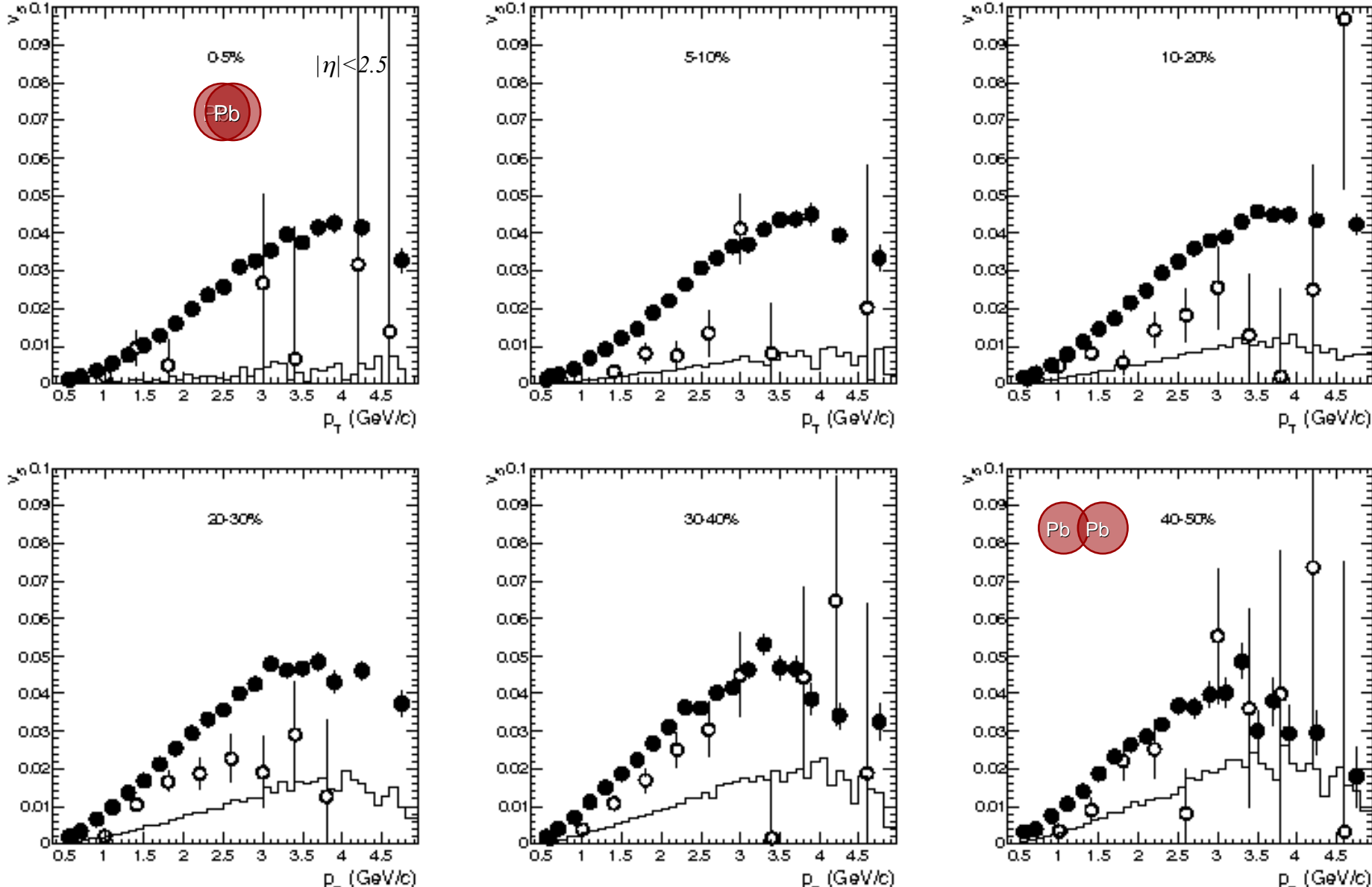
Quadrangular flow of inclusive charged hadrons



Closed circles: ATLAS data $v_4\{\text{EP}\}$ (*PRC 86 (2012) 014907*);

histograms and open circles: HYDJET++ (“true” $v_4(\psi_2)$ & $v_4\{\text{EP}\}$)

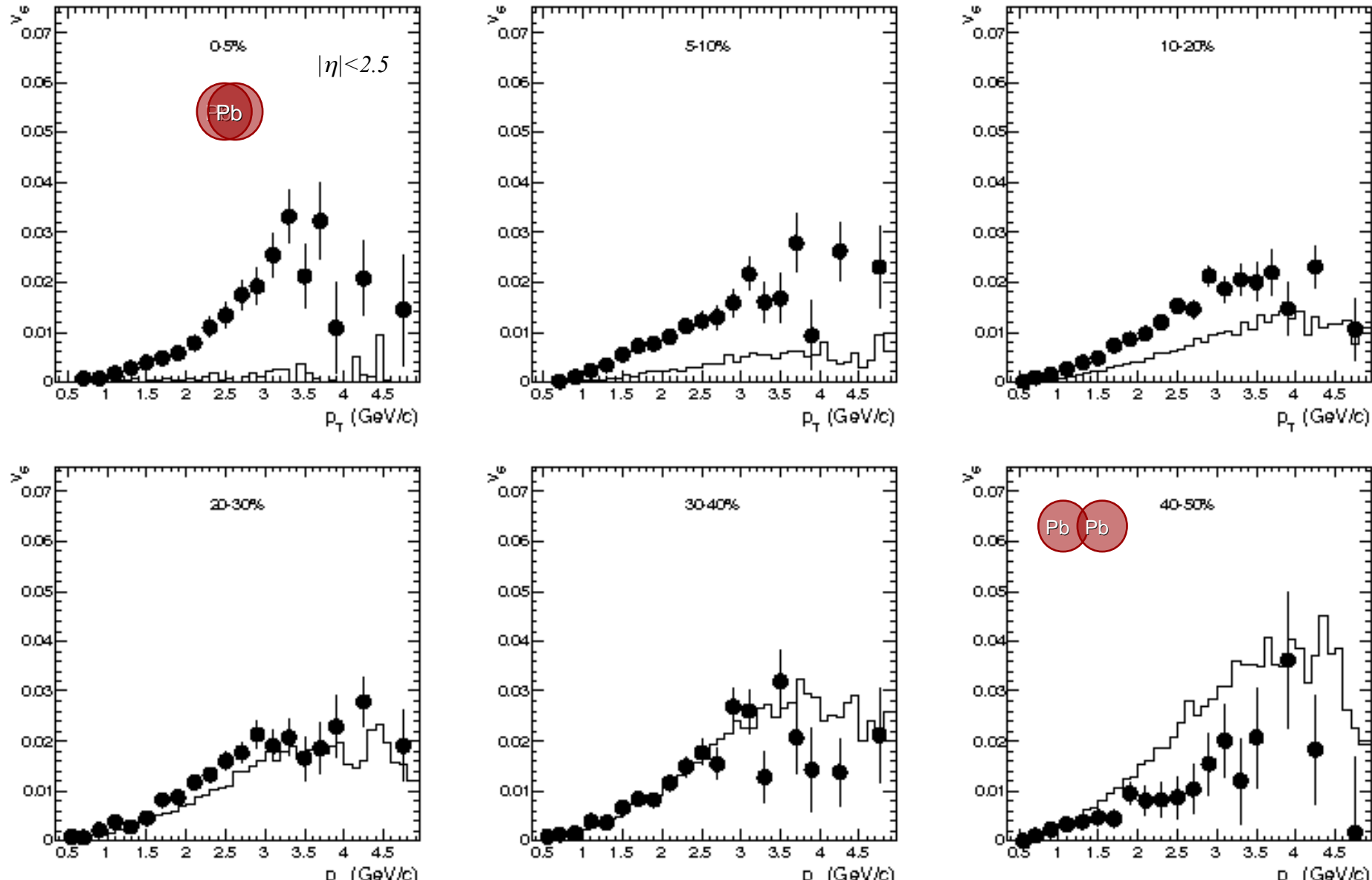
Pentagonal flow of inclusive charged hadrons



Closed circles: ATLAS data $v_5\{\text{EP}\}$ (*PRC 86 (2012) 014907*);

histograms and open circles: HYDJET++ (“true” $v_5(\psi_3)$ & $v_5\{\text{EP}\}$)

Hexagonal flow of inclusive charged hadrons

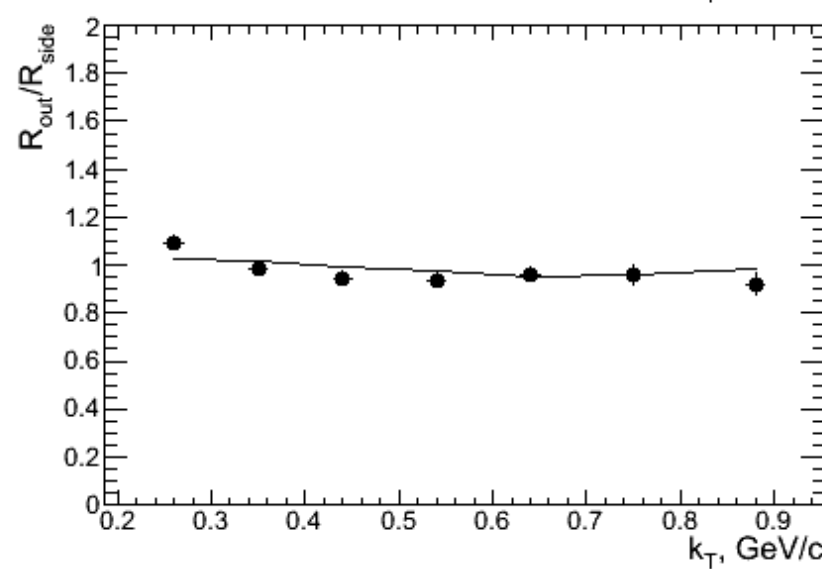
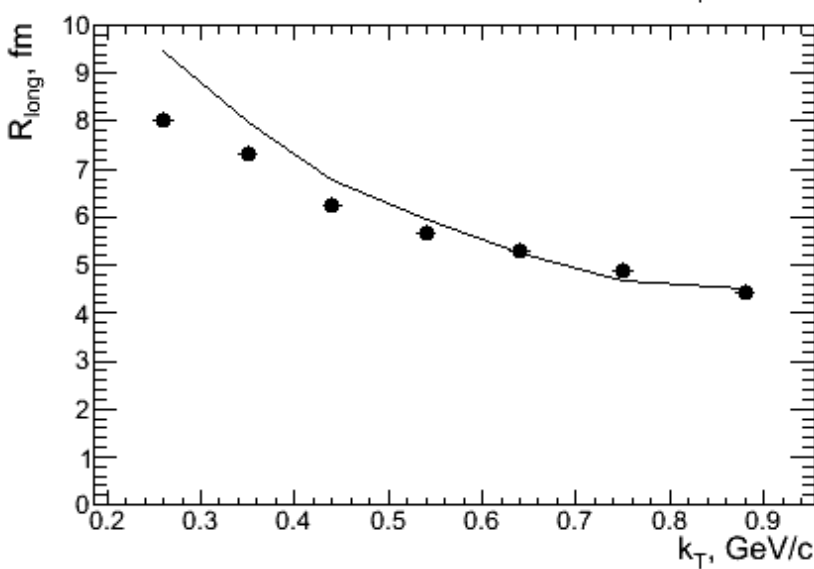
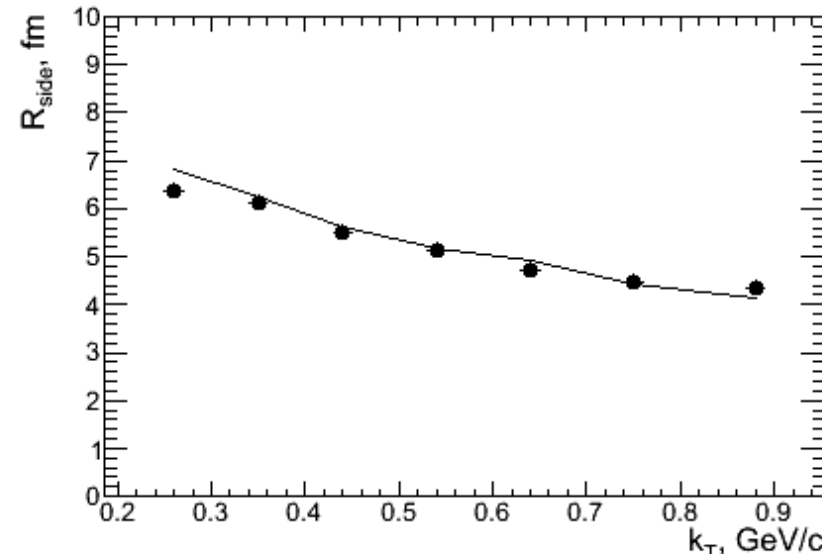
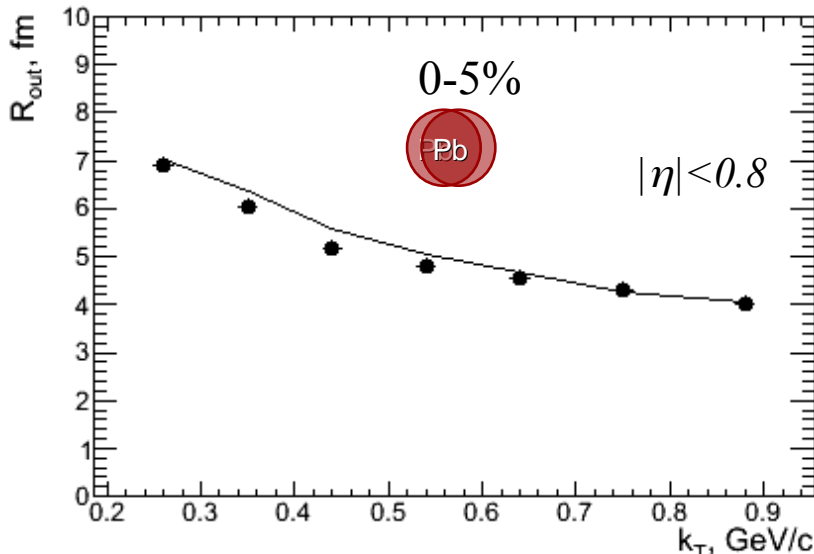


Closed circles: ATLAS data $v_6\{\text{EP}\}$ (*PRC 86 (2012) 014907*);

histograms: HYDJET++ (“true” $v_6(\psi_2)$)

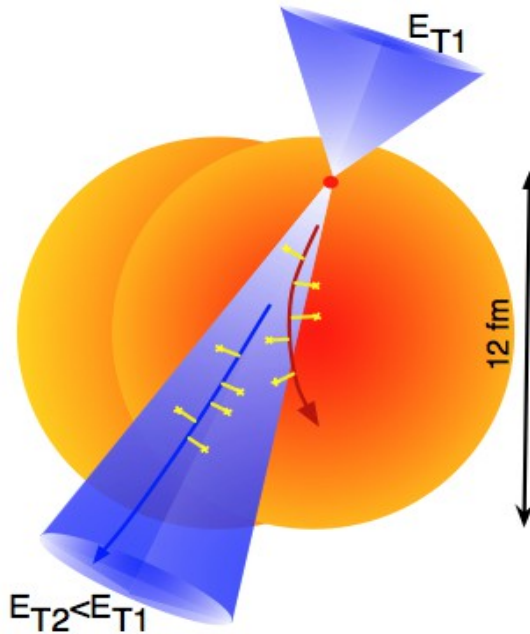
Femtoscopic momentum correlations (pion pairs)

$$CF = 1 + \lambda \exp(-R_o^2 q_o^2 - R_s^2 q_s^2 - R_l^2 q_l^2 - 2R_{ol}^2 q_o q_l)$$



Points: ALICE data (*PLB 696 (2011) 328*), histograms: HYDJET++

One of first new LHC results from lead-lead collisions at $\sqrt{s}=2.76$ A TeV was the observation of transverse energy asymmetry for dijet production in most central events. It is interpreted as a signal of partonic jet absorbtion in hot quark-gluon matter.



$$A_J = \frac{E_T^{j1} - E_T^{j2}}{E_T^{j1} + E_T^{j2}}$$

